BEHAVIOR OF TRANSMITTED WAVE IN GAIN MEDIA

BY

ABDALLAH MUHAMMAD AL ZAHRANI

A Thesis Presented to the

DEANSHIP OF GRADUATE STUDIES

KING FAHD UNIVERSITY OF PETROLEUM & MINERALS

DHAHRAN, SAUDI ARABIA

In Partial Fulfillment of the

Requirements for the Degree of

MASTER OF SCIENCE

In

PHYSICS

JUNE 1, 2005

KING FAHD UNIVERSITY OF PETROLEUM & MINERALS

DHAHRAN 31261, SAUDI ARABIA

DEANSHIP OF GRADUATE STUDIES

This thesis written by

ABDALLAH MUHAMMAD AL ZAHRANI

Under the supervision of his thesis Advisor and approved by his Thesis Committee, has been presented to and accepted by the Dean of Graduate Studies, in partial fulfillment of the requirement for the degree of

MASTER OF SCIENCE IN PHYSICS

Thesis Committee

Dr. Houcine Bahlouli (Chairman)

Dr. Abdulaziz Alhaidari (Co-Chairman)

Dr. Harry Mavromatis (Member)

Dr. Saeed Alamoudi (Member)

Dr. Abdullah Al-Sunaidi (Member)

Dr. Ali Al-Shukri
Department Chairman

Dr. Mohammad Al-Ohali
Dean of Graduate Studies

Date: June 1, 2005

I would like to dedicate my thesis to

my parents and grandmother

my sisters

my brothers

and my nieces

ACKNOWLEDGEMENT

Acknowledgement is due to King Fahd University of Petroleum & Minerals for supporting this research.

I wish to express my appreciation to my supervisors: Professor Houcine Bahlouli and Associate Professor Abdulaziz Alhaidari. I also wish to thank the members of my thesis committee: Professor Harry Mavromatis, Dr. Saeed Alamoudi and Dr. Abdullah AlSunaidi.

I would like to acknowledge the faculty members who offered technical support to me as well: Dr. Muhammad AlSunaidi, Dr. Rajai Alassar, Dr. Abdulaziz Aljalal and in particular Mr. Ezzat Abu-Azzah.

I would like to express very special acknowledgement to my mother and my brothers Tariq and Ali for computer and softwares supplies.

Finally I want to thank all of my colleagues for the valuable suggestions and fruitful discussions.

TABLE OF CONTENTS

LIST OF FIGURES

THESIS ABSTRACT

NAME OF STUDENT : ABDALLAH MUHAMMAD AL ZAHRANI

TITLE OF STUDY : BEHAVIOR OF TRANSMITTED WAVE IN GAIN MEDIA

MAJOR FIELD : PHYSICS

DATE OF DEGREE : JUNE 1, 2005

In this study, the behavior of transmitted waves (electromagnetic and quantum) is studied in gain (amplifying) media using complex media characteristics representation. The time-independent and time-dependent wave equations (electromagnetic and Schrödinger), that show contradictory results for the behavior of transmitted waves in gain media, are used to study the transmission comparatively. The contradiction between the results of the time-independent and time-dependent wave equations is studied and correlated to the resonance poles of the reflectance and transmittance. A first successful explanation for the paradoxical results of the time-independent and time-dependent wave equations is presented in this study.

MASTER OF SCIENCE DEGREE

KING FAHD UNIVERSITY OF PETROLEUM AND MINERALS

Dhahran, Saudi Arabia

JUNE 1, 2005

ملخص الرسالة

الاسم: عبد الله محمد إبراهيم الزهراني

عنوان الرسالة: سلوك الموجات النافذة في أوساط التكبير

التخصص: الفيزياء

تاريخ التخرج: ٢٣ ربيع الثاني ١٤٢٦

في هذا البحث تم دراسة سلوك الموجات (الكهرومغناطيسية والكمية) النافذة من أوساط التكبير باستخدام خصائص مركبة لتمثيل هذه الأوساط. لدراسة الموجات النافذة من أوساط التكبير تم استخدام معادلات الموجات (الكهرومغناطيسية والكمية) المعتمدة و اللا معتمدة على الزمن، و التي تعطي نتائج متناقضة لسلوك هذه الموجات. لحل ذلك التناقض بين نتائج معادلات الموجات المعتمدة و اللا معتمدة على الزمن، تم دراسة النقاط التي يحدث عندها انعكاسية أو نفاذية لانهائية عند استخدام معادلات الموجات اللا معتمدة على الزمن وربط التناقض في النتائج بهذه النقاط. وقد قدم تفسير ناجح للتناقض بين نتائج معادلات الموجات المعتمدة و اللا معتمدة على الزمن في أوساط التكبير لأول مرة في هذه الرسالة.

MASTER OF SCIENCE DEGREE

KING FAHD UNIVERSITY OF PETROLEUM AND MINERALS

Dhahran, Saudi Arabia

JUNE 1, 2005

CHAPTER 1

1. INTRODUCTION

In quantum and classical systems, scattering occurs when an incident wave experiences a change in the medium of propagation. In the case of electromagnetic (EM) waves, passive optical media are characterized by the real and positive quantities, the permittivity ε and the permeability μ. The magnetic properties of the system will not be taken into consideration in this work and hence we will set the permeability equal to unity in this work unless stated otherwise. In the case of matter waves, a passive medium is represented by a real potential V that can be positive or negative. In the case of active media (absorbing or amplifying), the parameters that represent different media are complex. For the EM waves, $\varepsilon \to \varepsilon' - i\,\varepsilon''$, where positive ε'' represents amplification and negative ε'' represents absorption (ε' and ε'' are real). For matter waves, $V \to V' + iV''$, where positive V'' yields amplification and negative V'' yields absorption (V' and V'' are real). Unlike in the case of light where the number of photons is not conserved, amplification in the case of particles is not physical since there is a restricting conservation law [4]. However, amplification of matter waves is one of the hottest contemporary research topics [5].

In the following chapters, the reflectance R and transmittance T in gain media (amplifying scattering media) will be calculated using the time-independent and time-dependent wave equations. Gain media will be represented by the complex parameters stated above. Moreover, the effects of different parameters of the scattering media and waves on *R* and *T* will be studied.

A generic picture of a gain system is shown in figure 1.1. Intuitively, as the length *L* of the gain medium or intensity of the gain increases, it is believed confidently that the transmitted wave will be further amplified. The transmittance for the system shown in figure 1.1 was calculated from the two time-independent wave equations analytically,

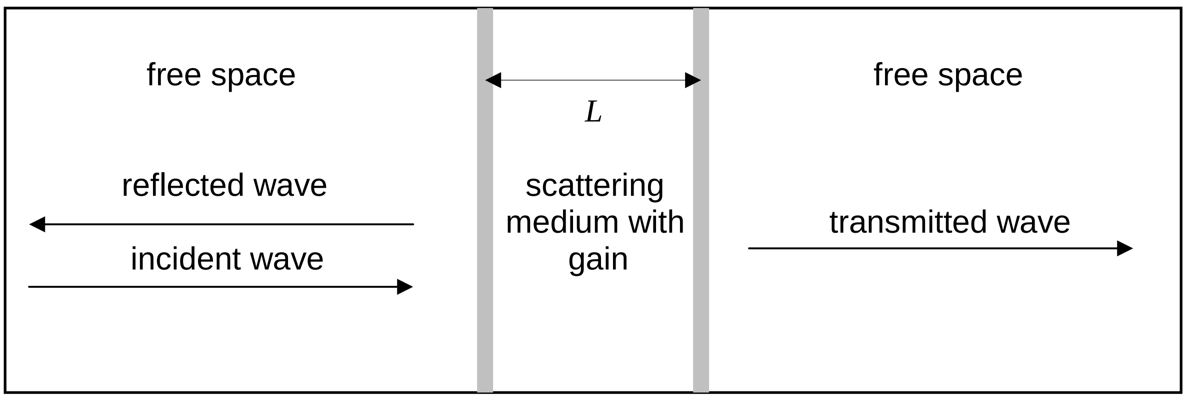

Figure 1.1: A generic picture of a gain system.

the Schrödinger and the EM wave equations, using the complex media parameters. The results were inconclusive. Gain was found to suppress wave propagation beyond some critical values of the parameters of the gain medium (length or gain intensity) as if the gain converts to loss as illustrated in figures 1.2 and 1.3. These results were reported in the literature by Soukoulis et al and others [1-3]. Actually it was generally shown by Beenakker et al. [9] that there is a dual symmetry between absorption and amplification for the propagation of radiation through a disordered medium with a complex dielectric constant. Nevertheless, the problem has to be looked at from another point of view to resolve the debate, namely, from the time-dependent wave equations.

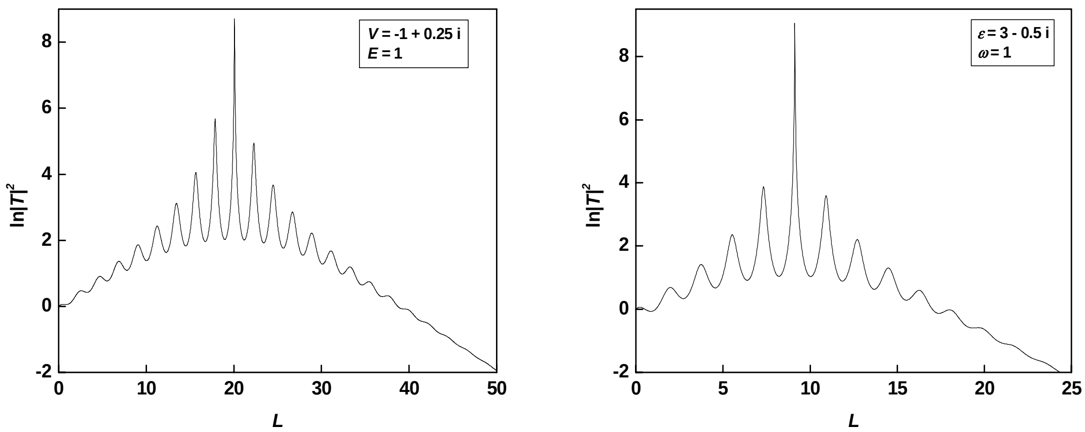

Figure 1.2: $\ln|T|^2$ **vs. gain medium length for the time-independent Schrödinger (left) and EM (right) wave equations.**

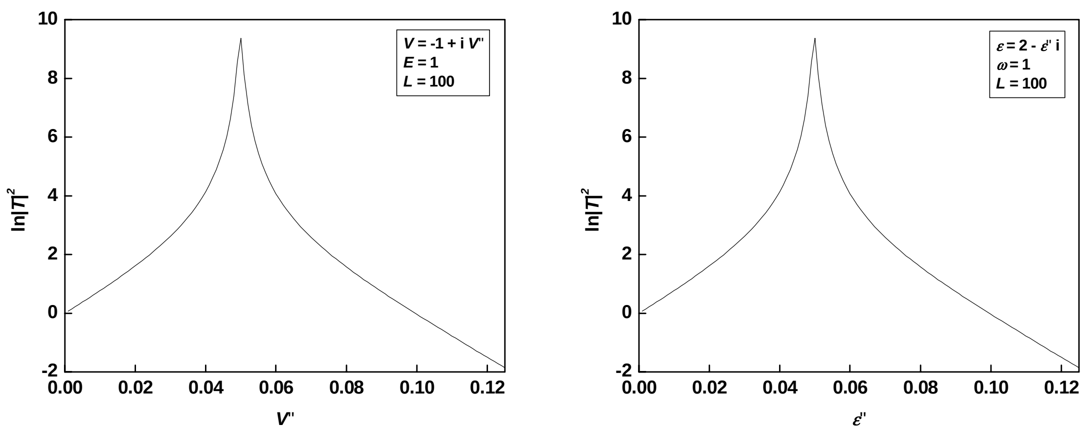

Figure 1.3: $\ln|T|^2$ **vs. gain intensity for the time-independent Schrödinger (left) and EM (right) wave equations.**

As was stated above, a clue to the resolution of this dilemma may come from the time-dependent wave equations. Again, intuition tells us that as the length L of the gain medium or the gain intensity increases, the transmitted wave will, with no doubt, be amplified more. The transmittance for the system shown in figure 1.1 was calculated numerically using the Finite Difference method for the two time-dependent wave equations (the Schrödinger and EM wave equations). The results showed no wave suppression in gain media, as intuitively expected, in accordance with the results reported in the literature [1-3]. Moreover, it was found that there are three main scenarios for the transmitted waves in gain media as shown in figure 1.4. At some critical gain intensity (V'' or ε'') or critical gain medium length L (of course the two parameters are dependent), wave outflow from the ends of the gain medium and wave amplification cancel each other. The gain medium serves as an everlasting wave source sending waves of finite and stable intensity as transmissions and reflections continuously. In that case the gain system is critical. Above this critical amplification threshold the system is overcritical and undercritical below it [1-3]. Accordingly, the output when the system is critical or overcritical will be infinite as time $t \to \infty$ and no finite stationary solution will exist.

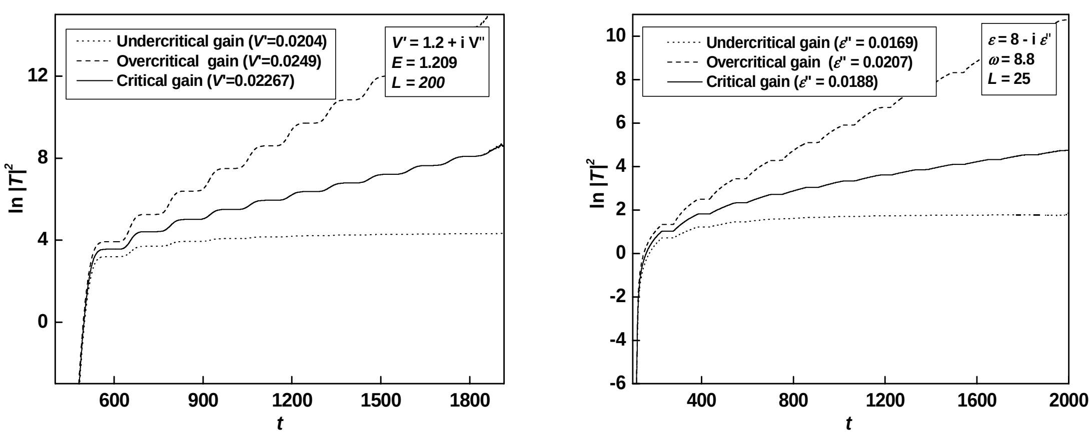

Figure 1.4: $\ln|T|^2$ **vs. time with three different gain intensities for the time-dependent Schrödinger (left) and EM (right) wave equations.**

Thus our work above confirmed the paradoxical results of the time-independent and time-dependent wave equations in gain media. The optical transmission through a segment of complex dielectric material [12] or the analogous electronic transmission through a complex scattering potential [3] exhibited a transition from amplification to absorption at a critical value of the gain intensity or gain medium length when treated using the time-independent wave equations. However, when the time-dependent wave equations were solved for the gain medium, no region of absorption was observed [1-3] even for critical systems. Soukoulis et al. [2-3] correctly pointed out the nature of the discrepancy between the time-dependent and the time-independent wave equations. However, there was no satisfactory explanation of the origin of this apparent paradox prior to this work [1].

It is worth mentioning that the time-independent EM wave equation was successful when used to predict the lasing modes by locating the poles in the complex frequency plane. It was also used to examine the spontaneous emissions below the lasing threshold in distributed feed back semiconductor lasers. [2]

A complete treatment of wave propagation in gain media can be achieved, in our view, by constructing the time-dependent solution from the whole spectrum of the time-independent solutions. Thus, both the discrete and continuous spectra should be included in the analysis similar to the approach of Hammer et al. [18] in dealing with the general solution of Schrödinger equation. The general solution in this case reads

$$\phi(x,t) = \int_{-\infty}^{+\infty} \frac{d\omega}{2\pi} f(\omega) g(x,\omega) e^{i\omega t} + \sum_n c_n g_n(x,\omega_n) e^{i\omega_n t} = \oint \frac{dz}{2\pi} f(z) g(x,z) e^{izt} \qquad (1.1)$$

Where $f(\omega)$ and c_n coefficients are determined from the initial value of $\phi(x,0) = h(x)$. In the last integral one has to choose a complex contour that will reflect the physical situation at hand. Keeping in mind that $g(x,\omega)$ and $g_n(x,\omega_n)$, solutions of the time-independent equation, are not orthonormal to each other because the operator is not Hermitian due to its complex nature in gain media. We believe that it will not be an easy task to determine analytically or numerically $f(\omega)$ and c_n, given $h(x)$.

In this work, we propose a new approach to explain the origin of the discrepancy between the results of the time-independent and time-dependent wave equations. Since the above mentioned problem seems to be common to both the EM and Schrödinger wave equations we try to keep this parallelism in our analysis setting aside the issue of practical relevance for electronic systems mentioned above [4]. In optical systems one can phenomenologically understand the increase of light intensity due to an increase in photons by means of coherent amplification, as by stimulated emission of radiation in an active lasing medium. However, in electronic systems and due to particle number conservation one cannot imagine such a violation of current conservation.

The main idea proposed is to relate the origin of the instability and divergence of the solutions of both the Schrödinger and EM wave equations to the time-dependence factors $e^{-iEt/\hbar}$ and $e^{-i\omega t}$, respectively [1]. This means that when the eigenenergy or eigenfrequency of a stationary eigenstate becomes very close to a particular real resonance pole of the system in consideration, the eigenstate will become unstable and blow up. Therefore, the pole structure of the transmittance in the complex energy or frequency plane will be studied. The value of the intensity of the gain will be tuned till an eigenenergy or eigenfrequency under consideration in the lower half of the complex frequency or energy plane approaches the real frequency or energy axis and cross it to the upper half plane. We speculate that this cross-over at the critical value of the gain is the origin of the discrepancy between the time-independent and time-dependent behaviors of the transmitted wave in gain media.

CHAPTER 2

2. NUMERICAL METHODS

2.1. Finite Difference Methods

The finite difference methods are probably the most prevailing numerical methods used to solve partial differential equations. Although finite difference methods have reliable stability, they require long computation times to reach fine accuracy. In the finite difference methods, the derivatives in a differential equation are replaced by corresponding difference-quotient approximations [23].

The Taylor expansion of a function $f(x)$ about a point x_0 is

$$f(x_0+\delta x)=f(x_0)+f'(x_0)\delta x+\frac{1}{2}f''(x_0)\delta x^2+.......... \qquad (2.1)$$

Which can be rearranged and solved for $f'(x_0)$ to give

$$f'(x_0)=\frac{f(x_0+\delta x)-f(x_0)}{\delta x}-\frac{\delta x}{2}f''(x_0)+.......... \qquad (2.2)$$

In Eq. 2.2, the first derivative is approximated by the slope of the straight line connecting the points at x_0 and $x_0+\delta x$. Therefore this method is called the **forward-difference formula**. One can conclude from Eq. 2.2 that this approximation has a truncation error of the order δx when the second and other higher order derivative terms are ignored. Similarly, one can obtain another expression for the first derivative by replacing δx by $-\delta x$. This method is called the **backward-difference formula** since the first derivative is approximated by the slope of the straight line connecting the points at x_0 and at $x_0 - \delta x$. This method is expressed as

$$f'(x_0) = \frac{f(x_0) - f(x_0 - \delta x)}{\delta x} + \frac{\delta x}{2} f''(x_0) + \dots\dots\dots \tag{2.3}$$

Approximating second derivatives is also straight forward. Adding the Taylor expansions of $f(x_0 + \delta x)$ and $f(x_0 - \delta x)$ yields

$$f(x_0 + \delta x) + f(x_0 - \delta x) = 2f(x_0) + f''(x_0)\delta x^2 + \frac{\delta x^4}{12} f^{(4)}(x_0) + \dots\dots\dots \tag{2.4}$$

Rearranging Eq. 2.4 yields

$$f''(x_0) = \frac{f(x_0 + \delta x) - 2f(x_0) + f(x_0 - \delta x)}{\delta x^2} - \frac{\delta x^2}{12} f^{(4)}(x_0) + \dots\dots\dots \tag{2.5}$$

Ignoring the fourth and other higher order derivative terms leads to an approximation for the second derivative with a truncation error of the order δx^2. In general, one can find a difference-quotient approximation for any derivative from suitable Taylor expansions. In the coming sections, some finite difference methods for the time-dependent Schrödinger and EM wave equations will be introduced.

2.1.1. The Time-dependent Schrödinger Wave Equation

The time-dependent Schrödinger wave equation in one dimensions with a static potential $V(x)$ in a system of units in which $\hbar = 2m_e = 1$ (See the last section of this chapter), is written as

$$i\frac{\partial \psi'(x,t)}{\partial t} = -\frac{\partial^2 \psi'(x,t)}{\partial x^2} + V(x)\psi'(x,t) \tag{2.6}$$

where m_e is the electron mass.

Using the substitution $\psi'(x,t) \to e^{i\,V(x)}\psi(x,t)$ Eq. 2.6 becomes

$$\frac{\partial\psi(x,t)}{\partial t} = i\frac{\partial^2\psi(x,t)}{\partial x^2}. \tag{2.7}$$

The transformation above is performed in a region where $V(x)$ is constant over space (the scattering medium) so that all of its spatial derivatives vanish. The latter equation is simpler and very similar to the classical heat equation. The imaginary number i is ignored as it will not change the numerical solution method of the equation. It may be, for example, absorbed in *t*. Now, using Eq. 2.2 and Eq. 2.5 to approximate the derivatives one finds

$$\frac{\psi(x_i,t_j+\delta t)-\psi(x_i,t_j)}{\delta t} = \frac{\psi(x_i+\delta x,t_j)-2\psi(x_i,t_j)+\psi(x_i-\delta x,t_j)}{\delta x^2} \tag{2.8}$$

where *i* (this *i* is an index that is different from the imaginary number *i* that was ignored as stated above) is the spatial index that runs from 0 to N_x and *j* is the temporal index that runs from 0 to N_t. Since $x_i + \delta x = x_{i+1}$ and $t_j + \delta t = t_{j+1}$, Eq. 2.8 can be rewritten neatly as

$$\frac{\psi_i^{j+1}-\psi_i^j}{\delta t} = \frac{\psi_{i+1}^j - 2\psi_i^j + \psi_{i-1}^j}{\delta x^2}. \tag{2.9}$$

Now, rearranging Eq. 2.9 and solving for ψ_i^{j+1} yield the following difference equation

$$\psi_i^{j+1} = (1-2\lambda)\psi_i^j + \lambda\left(\psi_{i+1}^j + \psi_{i-1}^j\right) \tag{2.10}$$

where $\lambda = \delta t/\delta x^2$. This equation can be written in matrix form as follows

$$\Psi^j = A\Psi^{j-1} \tag{2.11}$$

where $\Psi^j = \left(\psi_1^j, \psi_2^j, ..., \psi_{N_x-1}^j\right)^t$ and *A* is a tridiagonal matrix that reads

$$A = \begin{pmatrix} 1-2\lambda & \lambda & 0 & \cdots & 0 \\ \lambda & \ddots & \ddots & \ddots & \vdots \\ 0 & \ddots & \ddots & \ddots & 0 \\ \vdots & \ddots & \ddots & \ddots & \lambda \\ 0 & \cdots & 0 & \lambda & 1-2\lambda \end{pmatrix} \tag{2.12}$$

It is important to recall that the boundary conditions impose that $\psi_0^j = \psi_{N_x}^j = 0$ for all *j*.

Eq. 2.11 is straightforward to solve. One needs to know Ψ^j to directly find Ψ^{j+1}. The truncation error in approximating the derivatives in this method is of the order $\delta x^2 + \delta t$. However, this method is a **forward-difference method** or **explicit method** which is **conditionally stable**. The condition of stability is $\lambda = \delta x^2 / \delta t \le 1/2$.

An alternative way to have an **unconditionally stable** method is to use a **backward-difference method** or **implicit** method. This can be achieved via using the backward-difference formula stated as Eq. 2.3 to approximate the time derivative instead of the forward-difference formula stated as Eq. 2.2. With this modification, Eq. 2.9 becomes

$$\frac{\psi_i^j - \psi_i^{j-1}}{\delta t} = \frac{\psi_{i+1}^j - 2\psi_i^j + \psi_{i-1}^j}{\delta x^2}. \tag{2.13}$$

Rearranging Eq. 2.13 yields the following equation

$$(1+2\lambda)\psi_i^j - \lambda\left(\psi_{i-1}^j + \psi_{i-1}^j\right) = \psi_i^{j-1}. \tag{2.14}$$

And in matrix notation

$$B\Psi^j = \Psi^{j-1} \tag{2.15}$$

where *B* is obtained by replacing λ with $-\lambda$ in Eq. 2.12 and reads

$$B = \begin{pmatrix} 1+2\lambda & -\lambda & 0 & \cdots & 0 \\ -\lambda & \ddots & \ddots & \ddots & \vdots \\ 0 & \ddots & \ddots & \ddots & 0 \\ \vdots & \ddots & \ddots & \ddots & -\lambda \\ 0 & \cdots & 0 & -\lambda & 1+2\lambda \end{pmatrix} \tag{2.16}$$

A disadvantage of using the implicit method is that matrix inversion is needed to obtain Ψ^{j+1} from Ψ^{j}, i.e.

$$\Psi^{j} = B^{-1}\Psi^{j-1}. \tag{2.17}$$

Eq. 2.15 can be solved using the **Crout Factorization** or the **SOR** (successive over relaxation) method which is more suitable for large N_x [23]. Like the explicit method, the truncation error in approximating the derivatives in this implicit method is of the order $\delta x^2 + \delta t$. This requires making $\delta t << 1$ especially for large N_t.

The solution to this shortcoming is the **Crank Nicolson** method in which the forward-difference method

$$\frac{\psi_i^{j+1} - \psi_i^{j}}{\delta t} = \frac{\psi_{i+1}^{j} - 2\psi_i^{j} + \psi_{i-1}^{j}}{\delta x^2} \tag{2.9}$$

and the backward-difference method stated as Eq. 2.13 advanced by one step in time

$$\frac{\psi_i^{j+1} - \psi_i^{j}}{\delta t} = \frac{\psi_{i+1}^{j+1} - 2\psi_i^{j+1} + \psi_{i-1}^{j+1}}{\delta x^2} \tag{2.18}$$

are averaged. The resultant equation is

$$\frac{\psi_i^{j+1} - \psi_i^{j}}{\delta t} = \frac{1}{2}\left(\frac{\psi_{i+1}^{j} - 2\psi_i^{j} + \psi_{i-1}^{j}}{\delta x^2} + \frac{\psi_{i+1}^{j+1} - 2\psi_i^{j+1} + \psi_{i-1}^{j+1}}{\delta x^2}\right). \tag{2.19}$$

Rearranging Eq. 2.19 and putting it in matrix notation one obtains

$$B'\Psi^{j+1} = A'\Psi^{j} \tag{2.20}$$

where A' and B' are like A and B but with λ being replaced with $\lambda/2$. The solution to the latter difference equation is obtained directly by inverting B'

$$\Psi^{j+1} = B'^{-1} A' \Psi^{j} \,. \tag{2.21}$$

The truncation error in approximating the derivatives in this method is of the order $\delta x^2 + \delta t^2$, which is very advantageous. Like the implicit method, the Crank Nicolson method is unconditionally stable.

2.1.2. The Time-dependent EM Wave Equation

The classical wave equation that is used to describe electromagnetic wave propagation reads in one dimension

$$\frac{\partial^2 W(x,t)}{\partial x^2} = \frac{1}{\upsilon^2} \frac{\partial^2 W(x,t)}{\partial t^2}$$

(2.22)

where $W(x,t)$ is the electric (or magnetic) field and υ is the speed of the wave in some medium (*c* in vacuum). To solve the EM wave equation one needs to know *W* and its first time derivative at the initial time. Let us denote the former by $f(x)$ and the latter by $g(x)$. Now, to approximate the solution of Eq. 2.22, the EM wave equation, using the finite difference method, the second derivatives are approximated using Eq. 2.5. The EM wave equation will then appear as

$$W_i^{j+1} - 2W_i^{j} + W_i^{j-1} = \upsilon^2 \frac{\delta t^2}{\delta x^2} \left(W_{i+1}^{j} - 2W_i^{j} + W_{i-1}^{j} \right). \tag{2.23}$$

Using $\lambda = \upsilon\, \delta t / \delta x$ and solving for W_i^{j+1} give

$$W_i^{j+1} = 2\left(1-\lambda^2\right)W_i^j + \lambda^2\left(W_{i+1}^j + W_{i-1}^j\right) - W_i^{j-1}. \tag{2.24}$$

To solve this difference equation, a relation between W_i^j and W_i^{j-1} must be stated. This relation can be supplied from the knowledge of $g(x)$. Approximating the first derivative, one can write

$$g(x) = \frac{\partial W(x,t_0)}{\partial t} = \frac{W_i^1 - W_i^0}{\delta t} - \frac{\delta t}{2}\frac{\partial^2 W(x,t_0)}{\partial t^2} + ... \tag{2.25}$$

By solving for W_i^1 and dropping the second and higher order derivatives terms one obtains

$$W_i^1 = W_i^0 + \delta t\, g(i\,\delta x). \tag{2.26}$$

Although simple, Eq. 2.26 has a truncation error of the order δt [23]. More complicated analysis can lead to an alternative expression which has a truncation error of the order δt^3 [23], it reads

$$W_i^1 = \left(1-\lambda^2\right)W_i^0 + \frac{\lambda^2}{2}\left(W_{i+1}^0 + W_{i-1}^0\right) + k\,g(i\delta x). \tag{2.27}$$

Eq. 2.24 can be written in matrix form as

$$\mathbf{W}^{j+1} = C\,\mathbf{W}^j - \mathbf{W}^{j-1} \tag{2.28}$$

with $\mathbf{W}^j = \left(W_1^j, W_2^j, ..., W_{N_x-1}^j\right)^t$ and C is a tridiagonal matrix that has the form

$$C = \begin{pmatrix} 2\left(1-\lambda^2\right) & \lambda^2 & 0 & \cdots & 0 \\ \lambda^2 & \ddots & \ddots & \ddots & \vdots \\ 0 & \ddots & \ddots & \ddots & 0 \\ \vdots & \ddots & \ddots & \ddots & \lambda^2 \\ 0 & \cdots & 0 & \lambda^2 & 2\left(1-\lambda^2\right) \end{pmatrix}. \tag{2.29}$$

The solution of Eq. 2.28 is straight forward since the relation between $W_i^{\,j}$ and $W_i^{\,j-1}$ is known. The truncation error in approximating the second derivatives in this method is of the order $\delta x^2+\delta t^2$. However, this explicit method is conditionally stable. It requires that $\lambda=\upsilon\,\delta t/\delta x\le 1$.

To obtain an implicit method for the EM wave equation, the spatial derivative is approximated at two different times separated by $2\delta t$. The difference equation will then take the form [24]

$$W_i^{\,j+1}-2W_i^{\,j}+W_i^{\,j-1}=\frac{\upsilon^2\,\delta t^2}{2\delta x^2}\left(W_{i+1}^{\,j+1}-2W_i^{\,j+1}+W_{i-1}^{\,j+1}+W_{i+1}^{\,j-1}-2W_i^{\,j-1}+W_{i-1}^{\,j-1}\right). \quad (2.30)$$

Rearranging, one finds the equation

$$\begin{aligned}&-\lambda^2W_{i+1}^{\,j+1}+2\left(1+\lambda^2\right)W_i^{\,j+1}-\lambda^2W_{i-1}^{\,j+1}\\&\qquad=4W_i^{\,j}+\lambda^2W_{i+1}^{\,j-1}-2\left(1+\lambda^2\right)W_i^{\,j-1}+\lambda^2W_{i-1}^{\,j-1}.\end{aligned} \quad (2.31)$$

In matrix notation

$$D\mathbf{W}^{j+1}=4\mathbf{W}^{j}+E \quad (2.32)$$

where D is obtained by replacing λ^2 by $-\lambda^2$ in C

$$D=\begin{pmatrix}2\left(1+\lambda^2\right) & -\lambda^2 & 0 & \cdots & 0\\ -\lambda^2 & \ddots & \ddots & \ddots & \vdots\\ 0 & \ddots & \ddots & \ddots & 0\\ \vdots & \ddots & \ddots & \ddots & -\lambda^2\\ 0 & \cdots & 0 & -\lambda^2 & 2\left(1+\lambda^2\right)\end{pmatrix} \quad (2.33)$$

and E contains all the $\mathbf{W}^{j-1}$ terms in the right hand side of Eq. 2.31. Again matrix inversion is required for the solution since the method used is implicit, and the relation between E and $\mathbf{W}^{j}$ can be obtained directly from Eq. 2.27. The truncation error in approximating the derivatives is not improved, however, this method is implicit and unconditionally stable.

2.1.3. Stability Criteria

2.1.3.1. Stability of an Explicit Method

The error in finite difference methods is not merely the truncation error in approximating the derivatives. Propagation of the initial errors must be taken into account [23]. Let us consider the explicit method for the Schrödinger equation that has, in matrix notation, the following finite difference form (the indices in this section will be in parenthesis to distinguish them from powers)

$$\Psi^{(j)} = A\Psi^{(j-1)} \qquad (2.11)$$

where A was defined above.

If the error present in the initial condition $\Psi^{(0)} = \left(f\left(x_1\right), f\left(x_2\right), ..., f\left(x_{N_x-1}\right)\right)^t$ at time t_0 is $e^{(0)} = \left(e_1^{(0)}, e_2^{(0)}, ..., e_{N_x-1}^{(0)}\right)^t$, then the error that will propagate to the next time step $\Psi^{(1)}$ will be of $Ae^{(0)}$. Therefore, one can write

$$\Psi^{(1)} = A\left(\Psi^{(0)} + e^{(0)}\right) = A\Psi^{(0)} + Ae^{(0)}. \qquad (2.34)$$

At the *n*th time step, the error in $\Psi^{(n)}$ initiated from $e^{(0)}$ will be of $A^n e^{(0)}$ [23]. Usually it is true that $n \gg 1$. Hence, the method will be stable if the initial error does not grow up with time or when $\left|A^n e^{(0)}\right| \le \left|e^{(0)}\right|$ or $\left|A^n\right| \le 1$. This is true for the matrix A if $\rho\left(A\right) \le 1$, where $\rho(A)$ is the **spectral radius** of the matrix *A* defined as its maximum eigenvalue. It can be shown that the eigenvalues of the matrix *A* are given by [23]

$$\mu_i = 1 - 4\lambda\left(\sin\frac{i\pi}{2N_x}\right)^2. \tag{2.35}$$

Then the expression for $\rho(A)$ will read

$$\rho(A) = \max_{1\le i\le N_x-1}\left|1 - 4\lambda\left(\sin\frac{i\pi}{2\,N_x}\right)^2\right| \le 1. \tag{2.36}$$

Or equivalently

$$0 \le \lambda\left(\sin\frac{i\pi}{2\,N_x}\right)^2 \le \frac{1}{2}. \tag{2.37}$$

At $i = N_x - 1$ and when $\delta x \to 0$ or $N_x \to \infty$, we have

$$\lim_{N_x\to\infty}\left[\sin\frac{(N_x-1)\pi}{2\,N_x}\right]^2 = 1. \tag{2.38}$$

Therefore, condition 2.37 will be satisfied if and only if $0 \le |\lambda| \le 1/2$. Henceforth, the explicit method defined by Eq. 2.11 will be stable only if

$$\delta t/\delta x^2 \le 1/2. \tag{2.39}$$

2.1.3.2. Stability of an Implicit Method

For the implicit method applied to Schrödinger equation that has, in matrix notation, the following finite difference form

$$B\,\Psi^{(j)} = \Psi^{(j-1)} \tag{2.15}$$

the error that will propagate from $\Psi^{(0)}$ to the next time step $\Psi^{(1)}$ will be of $B^{-1}\,e^{(0)}$. Then one can write

$$\Psi^{(1)} = B^{-1}\left(\Psi^{(0)} + e^{(0)}\right) = B^{-1}\,\Psi^{(0)} + B^{-1}\,e^{(0)}\,. \tag{2.40}$$

Hence the propagating error will be of $B^{-n}\,e^{(0)}$ at the *n*th time step. The method is generally stable if and only if $\left|B^{n}\right| = \rho(B) \geq 1$. The eigenvalues of the matrix *B* can be shown to read [23]

$$\mu_i = 1 + 4\lambda\left(\sin\frac{i\,\pi}{2\,N_x}\right)^2 . \tag{2.41}$$

And since the spectral radius $\rho(B)$ is the maximum eigenvalue, it will be always true that $\rho(B) > 1$. Therefore, the implicit finite difference method is unconditionally stable. The same argument can be applied to the other methods for the two wave equations introduced above to study their stabilities.

2.2. Practical Remarks on the Finite Difference Methods for the Wave Equations

In this section, the numerical methods presented in the previous section for each of the two time-dependent wave equations will comparatively discussed in details, their advantages, disadvantages and stabilities in the case of gain. The initial incident waveforms and the ways to implement them numerically will be discussed as well. Moreover, since the simulated system is finite, the issue of the end effects (reflections at the boundaries of the system) will be also investigated.

2.2.1. The Schrödinger Wave Equation

2.2.1.1. Methods Survey and Stability

In the previous section, three main finite difference methods for the Schrödinger equation were introduced, namely, the explicit, implicit and Crank Nicolson methods. The explicit method is not used in this work at all since it is conditionally stable and not very different from the implicit method. At the beginning of this work, the implicit method was used. Although it showed perfect stability in the case of scattering in gainless media and reliable stability even in gain media, it required long running time since δt had to be very small to reach practical accuracy. The method that was used in this work for the time-dependent Schrödinger equation was the Crank Nicolson method. It showed perfect stability in the case of gainless media and reliable stability in the case of gain media. Moreover, the Crank Nicolson method ensured the accuracy goal required within a relatively short running time. It is important to mention that even with unconditionally stable methods, the risk of instability is evident in the case of gain where the system blows up *numerically* from the gain medium. In certain critical gain media, *physical* blow up exists due to multiple reflections within the system. Thus, it is imperative to discriminate between the physical gain and the numerical instabilities. Fortunately, it is not difficult to judge whether the blow up is numerical or physical. In the case of the latter, the blow up is gradual, smooth and uniform. On the other hand, the numerical blow up is sudden and non uniform. Two examples of physical blow up are illustrated in figure 2.1 and the three main cases of the numerical blow up are shown in figure 2.2.

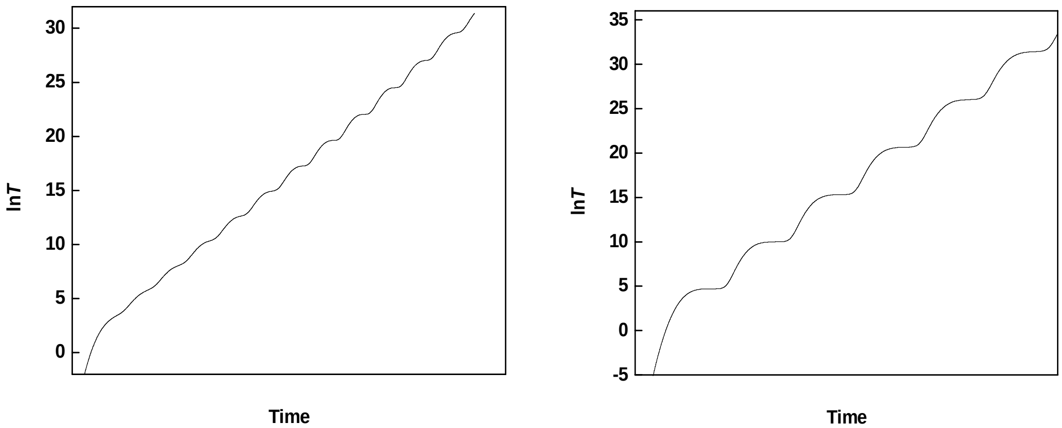

Figure 2.1: two examples physical blow up in critical gain systems due to physical amplification of the wave.

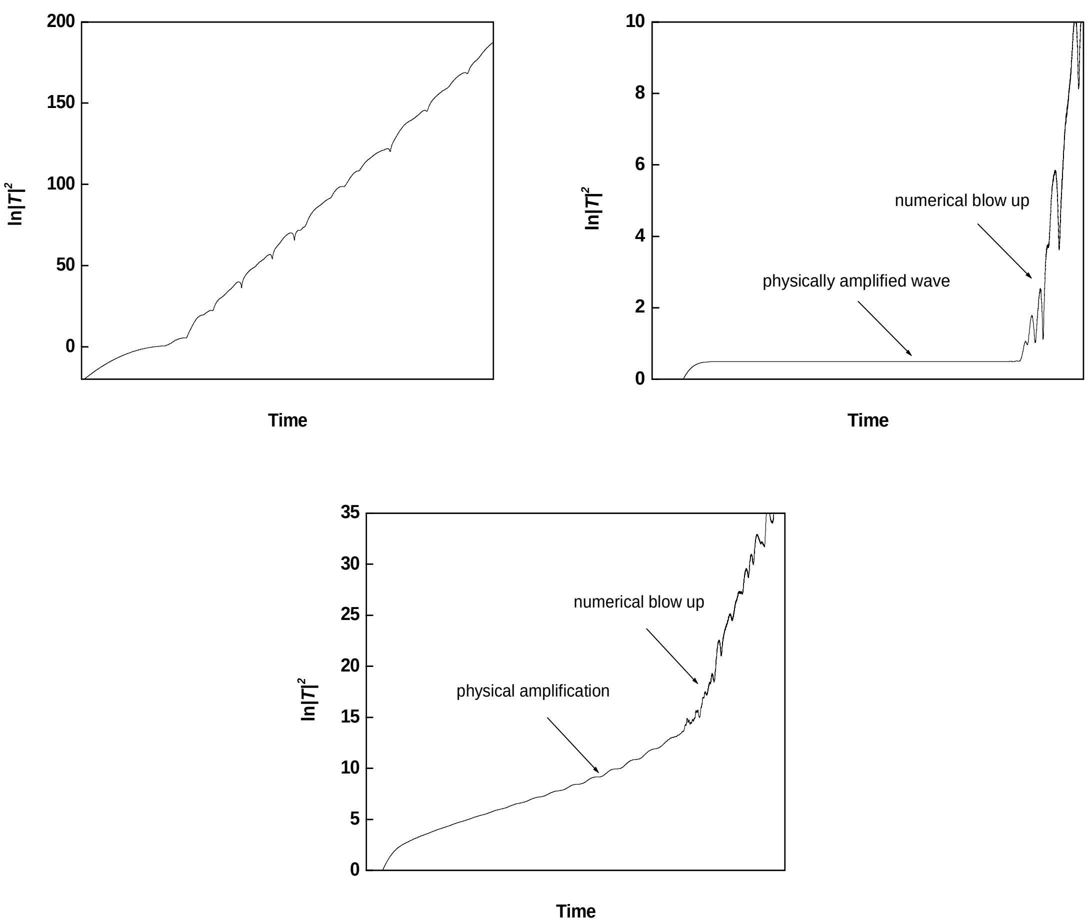

Figure 2.2: Different forms of numerical blow up for critical and undercritical gain systems.

There are several precautions to reduce the possibility of numerical instabilities. First of all, the incident wave should not exist initially in the gain medium. Moreover, the incident wave should be launched as far away as possible from the gain medium. Second, the larger the size of the gain medium is, the more stable the system will be. It should be kept in mind that the risk of numerical instabilities in gain media increases greatly with the gain intensity. Roughly speaking, the amplification is directly proportional to the gain media length and gain intensity. Consequently, we can simulate high amplification away from numerical instability by making the gain media larger and decreasing the gain intensity.

2.2.1.1 The Initial Waveform

The initial waveform used in the time-dependent Schrödinger wave equation was a Gaussian waveform centered at x_0 with a variance of σ and an average momentum of k_0

$$\psi(x,0) = e^{-\frac{(x-x_0)^2}{2\sigma^2}} e^{ixk_0}. \tag{2.42}$$

Since the Schrödinger equation describes the dynamics of a localized particle, it is not worth to discuss a plane wave as an initial waveform since it has lots of numerical difficulties that will be discussed later in the EM wave equation case.

2.2.1.2 The End Effects

Numerically, the reflectance *R* and transmittance *T* are calculated through the expressions [21]

$$|R(t)|^2 = \int_{-\infty}^{x_i} |\xi(x,t)|^2 \, dx \qquad (2.43)$$

$$|T(t)|^2 = \int_{x_f}^{\infty} |\xi(x,t)|^2 \, dx \qquad (2.44)$$

where $\xi(x,t)$ stands for the wave function for the two wave equations ($\psi(x,t)$ and $W(x,t)$), and x_i and x_f stand for the beginning and the end of the gain medium, respectively. The simulated system will always be finite. The waves in the simulated system will see its ends as an infinite potential barrier (infinite refractive index in the case of EM waves) and get totally reflected back to it. The end effects should be dealt with carefully. The most secure way to get rid of the end effects is to make the system large enough so that all calculations are performed before the reflected (or transmitted) waves by (or through) the gain media reach the ends of the system. This way the system will react exactly as if it were infinite. However, making the system very large is time consuming. It was found in this work that an alternative way to tackle the problem of the end effects is to allow the waves to get reflected back to the system by its ends. In this case the reflected waves by the ends of the system will be reflected back to it and join the other waves in it, and hence *R* and *T* will not be affected, as shown in figure 2.3. Moreover, this is also safe even in minute gain intensities as clearly indicated in figure 2.4. It is very important to mention that the waves reflected by the ends of the system must not reach the gain medium in which case the results will be erroneous. Absorbing boundaries can be used to prevent reflections at the ends, however, this will not be helpful in our problem since *R* and *T* will be diminished by the absorbing boundaries as the integrations in Eq. 2.43 and Eq. 2.44 will be diminished. Nevertheless, absorbing boundaries can be very helpful in deciding whether the system is critical or not.

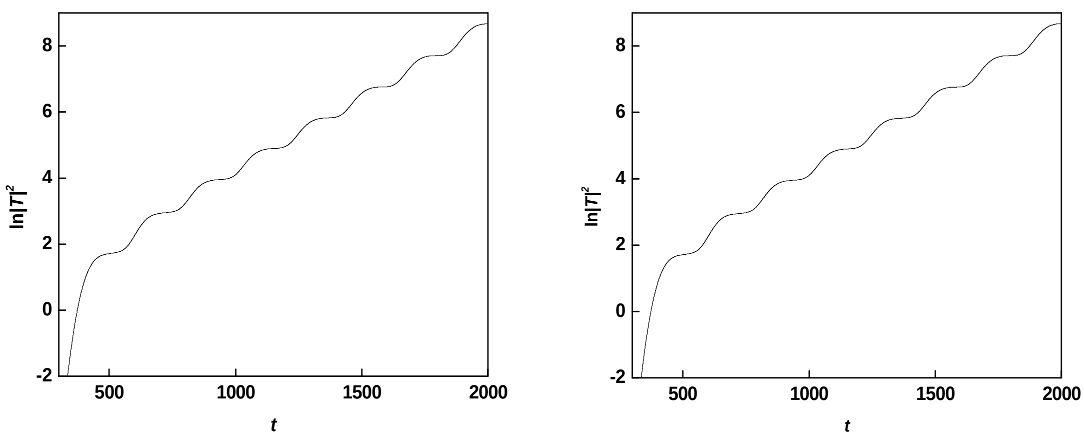

Figure 2.3: $\ln|T|^2$ **vs.** *t* **for the Schrödinger wave equation with intense gain for a very large system (left) and another system in which the reflections by the ends of the system are allowed (right).**

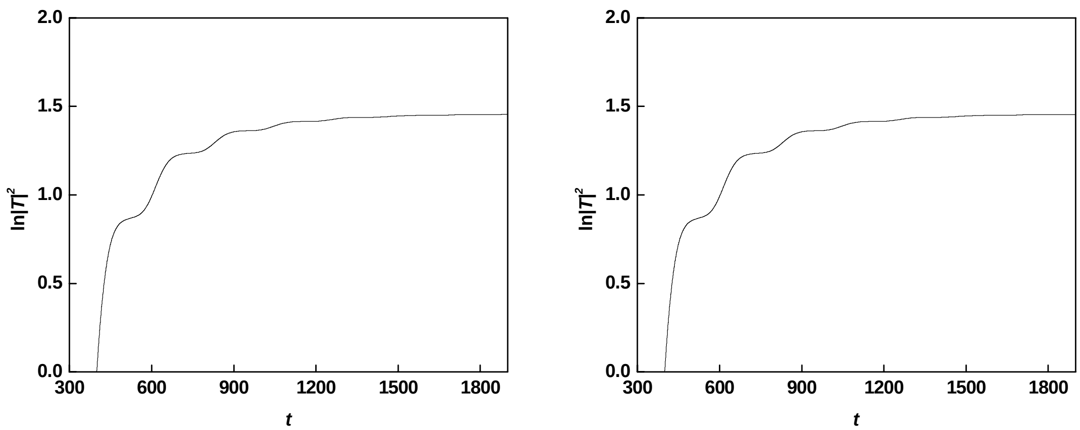

Figure 2.4: $\ln|T|^2$ **vs.** *t* **for the Schrödinger wave equation with minute gain for a very large system (left) and another system in which the reflections by the ends of the system are allowed (right).**

2.2.2. The EM Wave Equation

2.2.2.1. Methods Survey and Stability

As expected, the explicit method worked fine in the case of EM wave propagation and scattering in gainless media as long as the stability condition is met. Nonetheless, the explicit method showed poor stability in gain media although the stability condition was not violated. Results were stable only for too small gain intensities. Consequently, the explicit method was abandoned. On the other hand, the implicit method was very successful in handling gain and served quite well for practical gain intensities and hence was adopted overall this work.

2.2.2.2. The Initial Waveform

Two initial waveforms were used for the EM wave equation: a Gaussian pulse and plane wave. The Gaussian pulse was not quite suitable since its interaction with the scattering medium was very dependent on the variance of the pulse and we are interested in resonance effects. Therefore, plane waves were adopted in this work in the case of the EM waves. But the incident plane wave is not easy to implement numerically since it is infinite. Therefore, the initial plane wave should be initially truncated. However, truncation will make the wave have sharp edges at which the spatial derivatives may be very large. In that case, the higher derivative terms ignored in the difference-quotient approximation may cause some trouble. Alternatively, another technique to implement plane waves has been devised. The technique simply approximates a plane wave by the waveform

$$f(x)=\frac{e^{i\omega_0 x}}{1+e^{\frac{(x-x_0)^2}{a^2}-b^2}} \tag{2.45}$$

where a and b are real tunable parameters. It is interesting to note that when the exponential in the denominator is very small $f(x)$ reduces to a plane wave, and when it is very large $f(x)$ reduces to a Gaussian waveform. The width of this packet at half maximum is $2ab$. In addition, it was found numerically that its Fourier transform is almost exactly $\delta(\omega-\omega_0)$ for large a.

The first time derivative $g(x)$ described above plays an important role. It makes the initial wave move completely in one direction. However, one can safely set it equal to zero. In that case, the initial wave will split and travel in both directions. Consequently, the results will merely differ by a factor of half if the part of the wave traveling away from the scattering medium is excluded from the calculations.

2.2.2.3. The End Effects

Since $|R|^2$ and $|T|^2$ in the case of the EM wave equation are calculated using Eq. 2.43 and Eq. 2.44, the treatment of the end effects in the EM wave equation case is exactly similar to that in the Schrödinger wave equation case. In figures 2.4 and 2.5, $\ln|T|^2$ is calculated vs. time for a very large system in which the boundaries are not reached and another system in which the reflections by the boundaries are allowed, for large and small gain intensities.

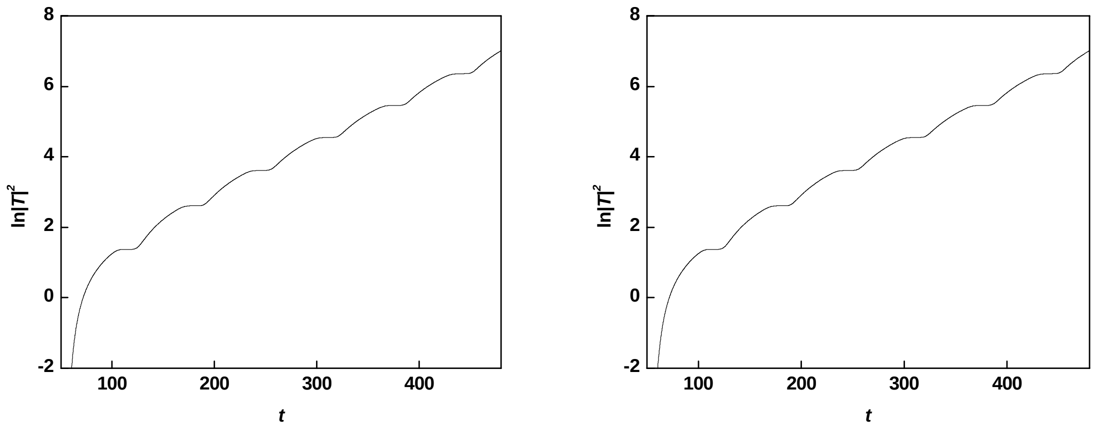

Figure 2.5: $\ln|T|^2$ **vs.** t **for the EM wave equation with intense gain for a very large system (left) and another system in which the reflections by the ends of the system are allowed (right).**

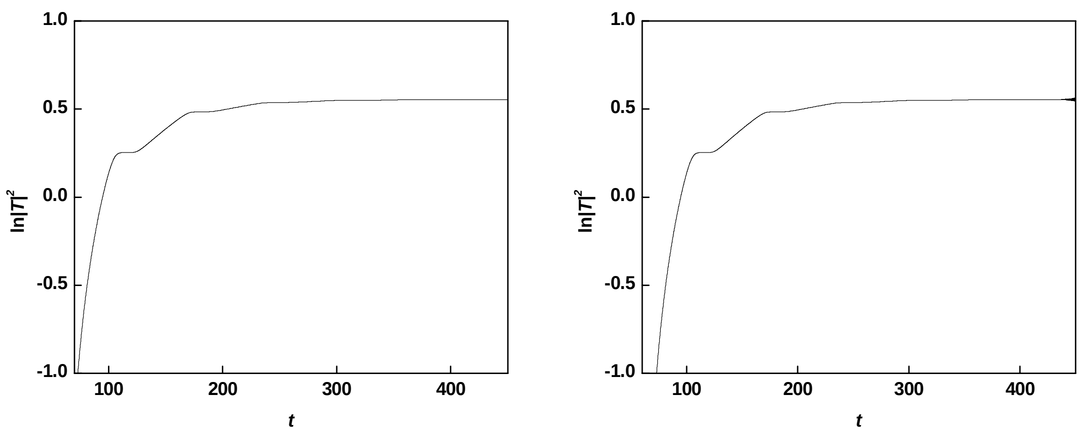

Figure 2.6: $\ln|T|^2$ **vs.** t **for the EM wave equation with minute gain for a very large system (left) and another system in which the reflections by the ends of the system are allowed (right).**

2.2.3. General Remarks

There are few general points that need to be mentioned before this numerical issue is closed. It is very important to use double precision when implementing the numerical algorithms using a programming language like FORTRAN. This is because in multiple arithmetical processes especially multiplications of extremely huge numbers by extremely small numbers, some significant figures may be lost. Although preferable, usually it is not very straightforward to increase the precision more than double precision in programming languages, which can be easily done in math softwares like *MATHEMATICA.* However, math softwares are too slow relative to programming languages.

A second important remark is that the space and time resolutions, δx and δt, should be chosen adequately small to make the simulation accurate enough, especially for long times simulations. There are several restrictive criteria on the space and time resolutions that are to be satisfied to obtain reliable accuracy [25]. However, the best way to determine the optimal resolution is to decrease the space and time steps until the solution becomes insensitive to the reduction of steps size. The stabilization of the results indicates that practically there is no loss of information due to space and time discretizations.

2.3. Complex Roots Finding

The well-liked method used to solve equations in one real variable is the Newton's iterative method. Fortunately, this method can be generalized and applied safely when the variable is complex.

Consider the Taylor expansion of the complex function $f(z)$, which has a root z_0, about $\bar{z}$, where $\bar{z}$ is an approximation to z_0. The expansion reads

$$f(z) = f(\bar{z}) + (z - \bar{z})\, f'(\bar{z}) + \frac{1}{2}(z - \bar{z})^2\, f''(\xi(z)) \tag{2.46}$$

where $\xi(z)$ lies between z and $\bar{z}$. At $z = z_0$ Eq. 2.46 becomes

$$0 = f(\bar{z}) + (z_0 - \bar{z})\, f'(\bar{z}) + \frac{1}{2}(z_0 - \bar{z})^2\, f''(\xi(z_0)). \tag{2.47}$$

Now assuming that $(z_0 - \bar{z})$ is very small enables one to drop the third term on the right hand side of Eq. 2.47 and write

$$0 \approx f(\bar{z}) + (z_0 - \bar{z})\, f'(\bar{z}) \tag{2.48}$$

Therefore an approximation can be obtained for z_0 from Eq. 2.48

$$z_0 \approx \bar{z} - \frac{f(\bar{z})}{f'(\bar{z})} \tag{2.49}$$

The assumption above requires that the initial approximation or guess $\bar{z}$ is good enough, i.e. close to the root z_0. To achieve more accuracy, successive iterations are made as follows

$$\bar{z}_n = \bar{z}_{n-1} - \frac{f(\bar{z}_{n-1})}{f'(\bar{z}_{n-1})} \tag{2.50}$$

here *n* is the number of iterations. However, it is not guaranteed that successive iterations will make the initial guess converge to the root. Further analysis can lead to alternative Newton's methods which are faster in convergence, but again the risk of divergence, or numerical overflow or underflow is evident.

Now, to make efficient use of the Newton's method for our work, two main obstacles must be overcome: the first is the numerical overflow or underflow and the second is blindness to multiple roots.

The first problem can be resolved through two operations. First, the value of the solution obtained from the Newton's method should be checked after every iteration whether it is inside some interval out which roots are not expected to occur or are not of interest or not. If the solution is outside the circle of interest, then the iterations are stopped. But, stopping the iterations may include solutions which are far away from the true roots. Therefore a second step is needed in which the solutions are checked.

The second problem can be solved by starting with different initial guesses. In the case of complex functions, an area of interest in the complex plane is scanned within some resolution depending on the equation to be solved.

2.4. Units Conversion

In many physical equations, constants that are extremely small or big are present, e.g. $\hbar^2$ and c^2. Therefore, the risk of numerical underflow or overflow is very probable. Henceforth, it is much securer to set such physical constants to unity or some appropriate value and then perform dimensional analysis to determine the new unit system in which those physical constant have the values to which they were set.

Starting with the Schrödinger equation, there are two numerically risky constants that should be disposed of, namely, $\hbar^2$ and the mass *m*, the mass of electron in our case.

Before performing dimensional analysis, let us first denote our energy unit by *E*, time unit by *T*, length unit by *L* and mass unit by *M*. In the analysis regarding the Schrödinger equation, numerically, it was found very helpful to use $\hbar = 2m = 1$. Then one can write,

$$\hbar = 1ET = N_\hbar \, J\, s \tag{2.51}$$

and

$$2m = 2N_m \, Kg = 1M = 1\frac{ET^2}{L^2} \tag{2.52}$$

where N_x is the S.I. numerical value of the constant *x* (i.e. without units), *J* denotes joules, *Kg* denotes kilograms and *s* denotes seconds. Solving for *E* and *L* gives a relation between the new units and the S.I. units in term of *T* as follows,

$$E = N_\hbar \, \frac{J\, s}{T} \tag{2.53}$$

$$L = \sqrt{\frac{N_\hbar}{2N_m}}\sqrt{\frac{J\, sT}{Kg}} = \sqrt{\frac{N_\hbar}{2N_m}}\sqrt{\frac{T}{s}}\, meter\,. \tag{2.54}$$

For $m = m_e$ and $T = 10^{-15}\, s$, we find that $E = 1.05457\times10^{-19}\, J = 0.658212\, eV$ and $L = 2.40591\text{Å}$. These units will be used overall this work for the Schrödinger wave equation. The difference between these units and the atomic units is that we have the freedom to choose the time unit. The atomic units can be obtained if the time unit was chosen as $T = 4.7^{-17}\, s$, then, one would have $E = 13.6\, eV$ and $L = 0.51\text{Å}$, as expected.

In the case of the EM wave equation, the speed of light c was set to unity. Consequently, dimensional analysis requires the following

$$c = N_c \frac{meter}{s} = 1\frac{L}{T} . \tag{2.55}$$

Therefore, there is complete freedom in choosing L and s. A good choice that satisfies Eq. 2.55 is $L = 300\, nm$ and $T = 1$ femtosecond. These units will be used overall this work for the EM wave equation.

CHAPTER 3

3. MAPPING BETWEEN THE SCHRÖDINGER AND ELECTROMANGTIC WAVE EQUATIONS

The propagation of the electromagnetic waves in a medium free of charges and currents is described by the EM wave equation

$$\nabla^2 W(r,t) = \mu\varepsilon \frac{\partial^2 W(r,t)}{\partial t^2} \tag{3.1}$$

where, for a uniform medium, the permeability μ and permittivity ε are generally space-time dependent and $W(r,t)$ stands for the electromagnetic fields, E or B. The time-independent wave equation for oscillatory electromagnetic fields of the form $W(r,t) = W(r)e^{i\omega t}$, becomes in one dimension

$$-\frac{\partial^2 W(x)}{\partial x^2} = \omega^2 \mu \varepsilon W(x). \tag{3.2}$$

The time-dependent EM and Schrödinger wave equations differ principally in the order of the time derivative. The chief physical difference between the two wave equations is that the former does not support bound states, as far as we know, while the latter does. The issue of light localization has been recently argued in the last decade. Rearrangement of the time-independent Schrödinger equation makes it read

$$(\nabla + E)\phi(r) = V(r)\phi(r). \tag{3.3}$$

On the other hand, the time-independent EM wave equation reads

$$\left(\nabla + \omega^2 \varepsilon(r)\right)\phi(r) = 0 \tag{3.4}$$

(here $\phi(r)$ is used in the two wave equations instead of $W(r)$ and $\psi(r)$). Since $\omega^2 = \zeta(E)$, where ζ is a function of energy E one can write Eq. 3.4 as

$$\left(\nabla + \zeta(E)\right)\phi(r) = \left(1 - \varepsilon(r)\right)\zeta(E)\phi(r). \tag{3.5}$$

Direct comparison between Eq. 3.3 and Eq. 3.5 proposes that the two wave equations will look similar if the potential V is energy dependent, i.e.

$$V(r,E) = \left(1 - \varepsilon(r)\right)\zeta(E). \tag{3.6}$$

Anyhow, more rigorous mapping between the two wave equations will be shown below. As discussed in chapter 1, the solution of the time-independent EM wave Eq. 3.2 above a certain gain threshold in an active medium is not appropriate for the description of wave propagation and that dual symmetry between absorption and amplification in such a medium is an artifact. Consequently, we attempted an alternative approach that was expected to shed some light on the origin of the problem. We did that by studying another time-independent but, presumably, equivalent system borrowed from relativistic field theory. In that alternative approach the property of the medium is equivalently represented by complex potentials that are taken to describe the non-hermitian dynamics of the relativistic fields. It goes as follows, Einstein's relativistic statement for material particles is $\vec{E}^2 = \mathcal{E}^2 - \vec{P}^2 c^2 = m^2 c^4$, where $\vec{E}$ is the four component energy vector $\vec{E} = \left(\mathcal{E}, c\vec{P}\right)$, $\mathcal{E}$ is the relativistic energy and $\vec{P}$ is the three-vector linear momentum. The operator equivalent statement is obtained by the operator substitution $\mathcal{E} \to i\hbar\frac{\partial}{\partial t}$ and $\vec{P} \to -i\hbar\vec{\nabla}$ giving the following relativistic wave equation

$$\left(\nabla^2 - \frac{1}{c^2}\frac{\partial^2}{\partial t^2}\right)\psi(t,r) = \left(\frac{mc}{\hbar}\right)^2 \psi(t,r) \tag{3.7}$$

which describes a free structureless particle of mass *m* whose dynamics is contained in the wave function $\psi(t,r)$. This is the celebrated Klein-Gordon (K-G) equation. For steady state description of particles, where $\psi(t,r) = \psi(r)e^{-i\mathcal{E}t/\hbar}$, it could be rewritten as the time-independent equation

$$\left(\nabla^2 + \frac{\mathcal{E}^2}{\hbar^2 c^2}\right)\psi(r) = \left(\frac{mc}{\hbar}\right)^2 \psi(r). \tag{3.8}$$

In the massless limit (when the Compton wavelength $\frac{\hbar}{mc}$ of the particle becomes very large) this equation looks very similar to Eq. 3.2 above. This, of course, is just the well-known wave-particle duality. Incidentally, using Eq. 3.7 we can study the effect of inertia on the transport properties of our system. Let us confine our discussion to problems in one dimension corresponding to the propagation of plane waves where Eq. 3.2 is rewritten as

$$\frac{dW^2(x)}{dx^2} + \omega^2 \mu(\omega,x)\varepsilon(\omega,x)W(x) = 0 \tag{3.9}$$

The corresponding K-G equation is

$$\frac{d^2\psi(x)}{dx^2} + \frac{\mathcal{E}^2\psi(x)}{\hbar^2 c^2} = \left(\frac{mc}{\hbar}\right)^2 \psi(x). \tag{3.10}$$

Now the effects of the property of the medium in Eq. 3.9, which is contained in the complex functions $\mu(\omega,x)$ and $\varepsilon(\omega,x)$, could be incorporated in Eq. 3.10 by an equivalent effect which is introduced in the form of potential interaction. Such interaction could be introduced in the K-G Eq. 3.10 in a gauge invariant way by rewriting it as follows [14]

$$\frac{d^2\psi(x)}{dx^2}+\frac{1}{\hbar^2c^2}\left[\mathcal{E}-V(x)\right]^2\psi(x)=\left(\frac{mc}{\hbar}\right)^2\psi(x) \tag{3.11}$$

where $V(x)$ is the time component of a vector potential whose space component is taken to vanish. This could also be generalized to include coupling to a space-time scalar potential $S(x)$ as follows [16, 17]

$$\left\{\frac{d^2}{dx^2}+\frac{1}{\hbar^2c^2}\left[\mathcal{E}-V(x)\right]^2-\frac{1}{\hbar^2c^2}\left[mc^2+S(x)\right]^2\right\}\psi(x)=0\,. \tag{3.12}$$

By now, for a given set of medium configuration, specified by $\varepsilon(\omega,x)$ and boundary conditions we choose the complex potentials $V(x)$ and $S(x)$ in Eq. 3.12 with m = 0 that will give the same electromagnetic wave equation, Eq. 3.9. The potentials so obtained will be our guide in writing the non-relativistic Schrödinger equation to give the quantum mechanical analogue of the wave propagation equation. It was hoped that this approach will shed light on some aspects of the problem that could help in the resolution of some of the discrepancies encountered. We start with a simplified problem where the medium is non-dispersive and the relative permeability μ is constant. Further simplification will also be introduced by choosing a uniform medium corresponding to complex but constant permittivity and potentials.

Let us consider the system that is shown in figure 4.5 (chapter 4). The parameters $(\varepsilon',\varepsilon'',V',V'',S',S'')$ are real. Eq. 3.9 gives in media I and III

$$\frac{d\,W(x)}{dx^2} + \omega^2 \; W(x) = 0 \tag{3.13}$$

And in medium II

$$\frac{d\,W(x)}{dx^2} + \omega^2 (\varepsilon' - i\,\varepsilon'')\, W(x) = 0 \tag{3.14}$$

On the other hand, Eq. 3.12 with m = 0 and $\mathcal{E} = \hbar\omega$, gives in media I and III

$$\frac{d\psi(x)}{dx^2} \; + \omega^2 \psi(x) \; = 0 \tag{3.15}$$

And in medium II

$$\frac{d\psi(x)}{dx^2} \; + \omega^2 \left[1 - 2\frac{1}{\hbar\omega} V + \frac{1}{\hbar^2 \omega^2} \left(V^2 - S^2 \right) \right] \; \psi(x) \; = 0 \tag{3.16}$$

Comparing Eq. 3.14 to Eq. 3.16, we obtain

$$\varepsilon' = 1 - 2\tfrac{1}{\hbar\omega} V' + \tfrac{1}{\hbar^2 \omega^2} \left(V'^2 - V''^2 - S'^2 + S''^2 \right) \tag{3.17}$$

$$\varepsilon'' = 2\tfrac{1}{\hbar\omega} V'' + 2\tfrac{1}{\hbar^2 \omega^2} \left(S'S'' - V'V'' \right) \tag{3.18}$$

Now since the medium is assumed to be non-dispersive (i.e., the permittivity is independent of the frequency ω) then we conclude that the constant potentials V and S in medium II should be proportional to ω. In other words the vector and scalar potentials in the Klein-Gordon equation are *energy dependent*. They should be proportional to E. Consequently, we write these potentials as

$$V \equiv \mathcal{E} v \,, \;\; S \equiv \mathcal{E} s \,, \tag{3.19}$$

where v and s are dimensionless parameters. Thus, we can now write

$$\varepsilon' = 1 - 2v' + v'^2 - v''^2 - s'^2 + s''^2 \tag{3.20}$$

$$\varepsilon'' = 2v'' + 2s's'' - 2v'v'' \tag{3.21}$$

It might be intuitively obvious that since μ is constant and the property of the optical medium is defined by the two permittivity parameters ε' and ε'' then it is sufficient to describe the corresponding K-G system by only one potential function with its two parameters (e.g. v' and v''). Thus, we take *S* = 0 in which case Eq. 3.20 and Eq. 3.21 will determine v' and v'' in terms of the parameters ε' and ε'' as follows

$$\left(1-v'\right)^2 = \frac{|\varepsilon'|}{2}\left[\pm 1 + \sqrt{1+\left(\varepsilon''/\varepsilon'\right)^2}\right], \text{ for } \pm\varepsilon' > 0 \tag{3.22}$$

$$v'' = \frac{\varepsilon''/2}{1-v'} \tag{3.23}$$

Solving Eq. 3.22 and Eq. 3.23 gives

$$V = \mathcal{E}\left[v'(\varepsilon',\varepsilon'') + \mathrm{i}v''(\varepsilon',\varepsilon'')\right]. \tag{3.24}$$

That is, in our investigation of the wave propagation through the quantum mechanically equivalent system we will take the potential in the Schrödinger equation as $V = E\left(v + \mathrm{i}\, v''\right)$ when we try to resolve the paradoxical results described before, where *E* is the non-relativistic energy and v' and v'' are real potential parameters. This simplified analysis clearly shows the highly non-trivial nature of the equivalent potential representation.

It will be shown in the last section of chapter 5 that the Schrödinger equation with the described energy dependent potential yields resonance poles of the reflectance and transmittance similar to those of the reflectance and transmittance of the EM wave equation. It is the only case in which the poles of the reflectance and transmittance of the Schrödinger equation are aligned straightly in the complex *k*-plane similar to those of the reflectance and transmittance of the EM wave equation in the complex ω-plane. The problem of energy-dependent potentials is highly non-trivial problem which is a topic of interest on its own. The Schrödinger equation with energy-dependent potentials has been recently used in the description of heavy quark systems [26]. In chapter 5 where the subject of resonance poles is discussed, the poles of the reflectance and transmittance of the Schrödinger wave equation with potentials of various energy dependencies will be shown. It will be seen that the best mapping between the EM and Schrödinger wave equations is obtained through using an energy dependent potential with direct proportionality.

It is important to mention that the only help (in the problem of the paradoxical results introduced in chapter 1) presented through using an energy dependent potential with direct proportionality is that the resonance poles of the reflectance and transmittance of the Schrödinger wave equation could be studied analytically.

CHAPTER 4

4. TIME-DEPENDENT WAVE EQUATIONS

One of the corner stones of quantum mechanics is that the time development of the state function $\psi(x,t)$ for a particle or a system is described by the time-dependent Schrödinger equation [20]

$$i\hbar\frac{\partial}{\partial t}\psi(x,t)=\hat{H}\psi(x,t) \tag{4.1}$$

where the operator $\hat{H}$ is the Hamiltonian operator. In one dimension it takes the form

$$\hat{H}=-\frac{\hbar^2}{2m}\frac{\partial^2}{\partial x^2}+V(x)\,. \tag{4.2}$$

The axiom of Hermiticity may be replaced by the more physical condition of *space–time reflection symmetry* [29]. This is much related to this work as gain media are represented using a non-Hermitian Hamiltonian. To obtain the time-independent form of the Schrödinger equation we replace $\psi(x,t)$ in the time-dependent Schrödinger equation with $\psi(x)e^{-iE\,t/\hbar}$. Then Eq. 4.1 becomes

$$\hat{H}\psi(x)=E\psi(x) \tag{4.3}$$

where E is the energy of the system.

As mentioned in the last chapter, the propagation of electromagnetic waves in any medium is governed by the electromagnetic (EM) wave equation

$$\nabla^2W(r,t)=\mu\varepsilon\frac{\partial^2W(r,t)}{\partial t^2}\,. \tag{4.4}$$

Which reduces in one dimension to

$$\frac{\partial^2 W(x,t)}{\partial x^2} = \mu\varepsilon \frac{\partial^2 W(x,t)}{\partial t^2} \tag{4.5}$$

where $W(x,t)$ is the electric or magnetic field and μ and ε are the permeability and permittivity, respectively, that describe the medium of propagation. In analogy with the Schrödinger equation case, a time-independent version of the EM wave equation is obtained if we substitute $W(x,t)$ in the time-dependent wave equation with $W(x)e^{-i\omega t}$ as mentioned in the previous chapter. The new wave equation in any media will look like

$$-\frac{\partial^2 W(x)}{\partial x^2} = \omega^2 \mu\varepsilon W(x). \tag{4.6}$$

where ω is the frequency of the EM wave. In the coming sections the above two stationary wave equations will be used to study the problem of one-dimensional scattering through a gainless and gain media.

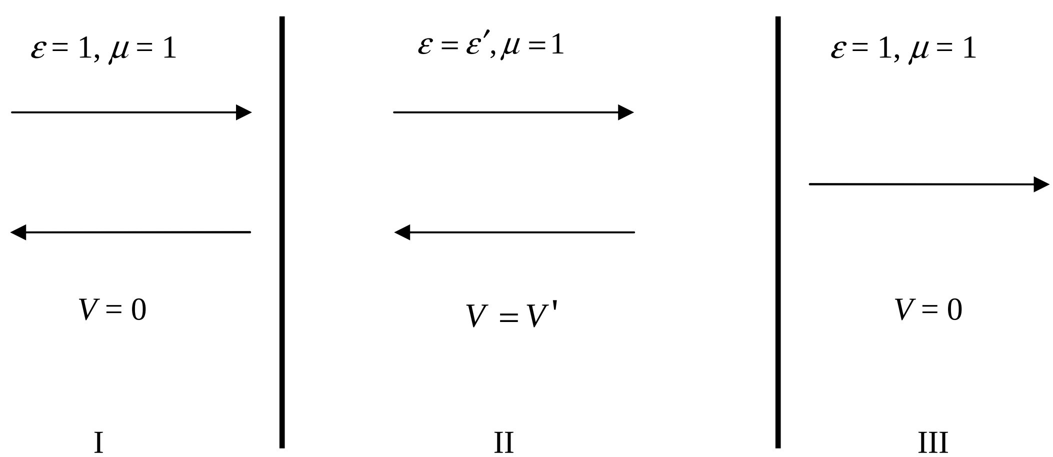

Figure 4.1: A one-dimensional scattering problem of an EM or quantum wave by a gainless scattering medium of length *L*.

4.1. One-Dimensional Scattering Through a Gainless Medium

Our aim now is to solve the time-independent wave equations for the simple scattering system depicted in figure 4.1 for any potential. The solutions of the time-independent wave equations in the three regions shown in figure 4.1 are, in the Schrödinger equation case

$$\psi(x)=\begin{cases} e^{ik_I x}+R\,e^{-ik_I x} & \text{I} \\ A e^{ik_{II} x}+B\,e^{-ik_{II} x} & \text{II} \\ T\,e^{ik_{III} x} & \text{III} \end{cases} \tag{4.7}$$

with $k=\sqrt{2m(E-V(x))}/\hbar$. And in the EM wave equation case, the solutions are

$$W(x)=\begin{cases} e^{i\sqrt{\varepsilon_I}x}+R\,e^{-i\sqrt{\varepsilon_I}x} & \text{I} \\ A e^{i\sqrt{\varepsilon_{II}}x}+B\,e^{-i\sqrt{\varepsilon_{II}}x} & \text{II} \\ T\,e^{i\sqrt{\varepsilon_{III}}x} & \text{III} \end{cases} \tag{4.8}$$

To obtain an expression for the transmittance *R* and reflectance *T*, one has to match the three solutions at the boundaries, $x=0$ and $x=L$, and match their derivatives as well. After doing that and solving for *R* and *T*, one obtains for the Schrödinger wave equation

$$R=V\frac{1-e^{2iL\sqrt{k^2-V}}}{e^{2iL\sqrt{k^2-V}}\left(k-\sqrt{k^2-V}\right)^2-\left(k+\sqrt{k^2-V}\right)^2} \tag{4.9}$$

$$T=\frac{4e^{-iL\left(k-\sqrt{k^2-Ve}\right)}k\sqrt{k^2-V}}{e^{2iL\sqrt{k^2-V}}\left(k-\sqrt{k^2-V}\right)^2-\left(k+\sqrt{k^2-V}\right)^2} \tag{4.10}$$

and for the EM wave equation

$$R=\frac{\left(e^{2iL\sqrt{\varepsilon}\omega}-1\right)(\varepsilon-1)}{e^{2iL\sqrt{\varepsilon}\omega}\left(\sqrt{\varepsilon}-1\right)^2-\left(\sqrt{\varepsilon}+1\right)^2} \tag{4.11}$$

$$T = \frac{4e^{2iL(\sqrt{\varepsilon}-1)\omega}\sqrt{\varepsilon}}{e^{2iL\sqrt{\varepsilon}\omega}\left(\sqrt{\varepsilon}-1\right)^2-\left(\sqrt{\varepsilon}+1\right)^2} \tag{4.12}$$

Simpler expressions can be obtained if one makes use of the conservation law $|R|^2+|T|^2=1$ [20]. However, in gain media, which are of interest to us in this study, this conservation law is violated. In figure 4.2, $|R|^2$ and $|T|^2$ are plotted for the Schrödinger and EM wave equations vs. the scattering medium length *L*. It is clear in these two figures that $|R|^2$ and $|T|^2$ always add to 1 as they should. The behaviors of $|R|^2$ and $|T|^2$ for the two wave equations are periodic in *L*. Moreover, the behaviors of $|R|^2$ and $|T|^2$ vs. potential in the case of the Schrödinger wave equation and vs. permittivity in the case of the EM wave equation are depicted in figures 4.3. It is obvious from figure 4.3 (left) that $|R|^2$ is zero when the potential is zero and approaches unity asymptotically, in contrast, $|T|^2$ is unity when the potential is zero and approaches zero asymptotically, which one should get. On the other hand, figure 4.3 (right) shows a periodic like behavior with permittivity change which is very interesting. Even for very large refractive index resonance transmission still can happen. Finally it is worth to study the behaviors of $|R|^2$ and $|T|^2$ vs. energy in the case of the Schrödinger wave equation and vs. frequency in the case of the EM wave equation. The results are shown in figure 4.4. From figure 4.4 (left), one can conclude that the dependences of $|R|^2$ and $|T|^2$ on the incident energy are roughly opposite to their dependences on the potential. On the other hand, figure 4.4 (right) shows periodic behavior but noticeably different form that of figure 4.3 (right).

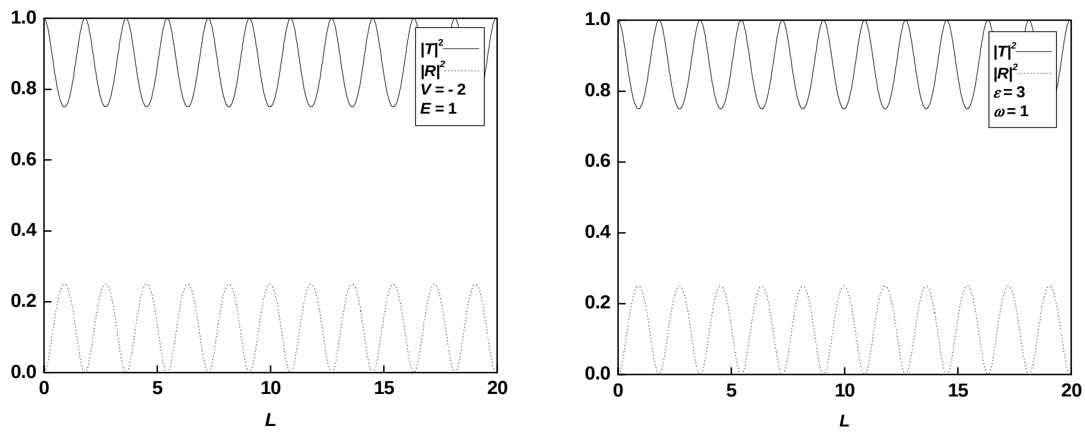

Figure 4.2: $|R|^2$ **and** $|T|^2$ **vs.** L **for the Schrödinger (left) and EM (right) wave equations.**

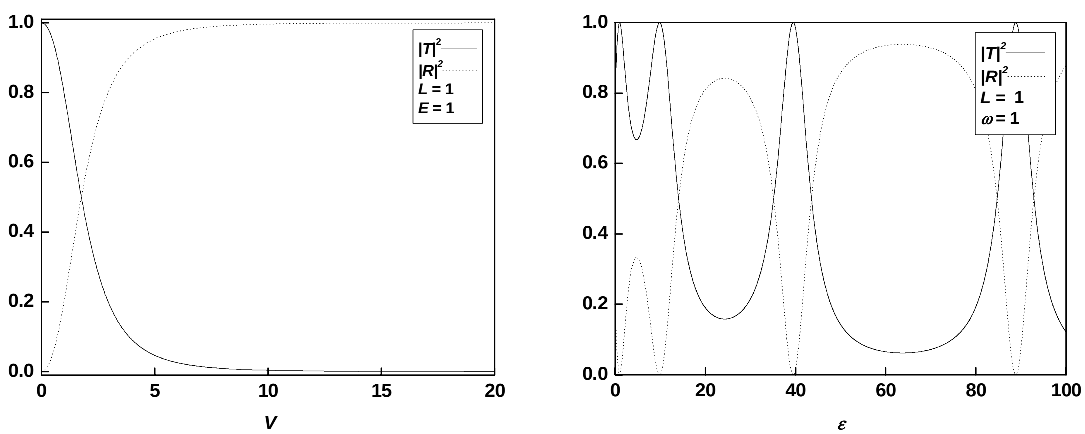

Figure 4.3: $|R|^2$ **and** $|T|^2$ **vs.** V **for the Schrödinger wave equation (left) and vs.** ε **for the EM wave equation (right).**

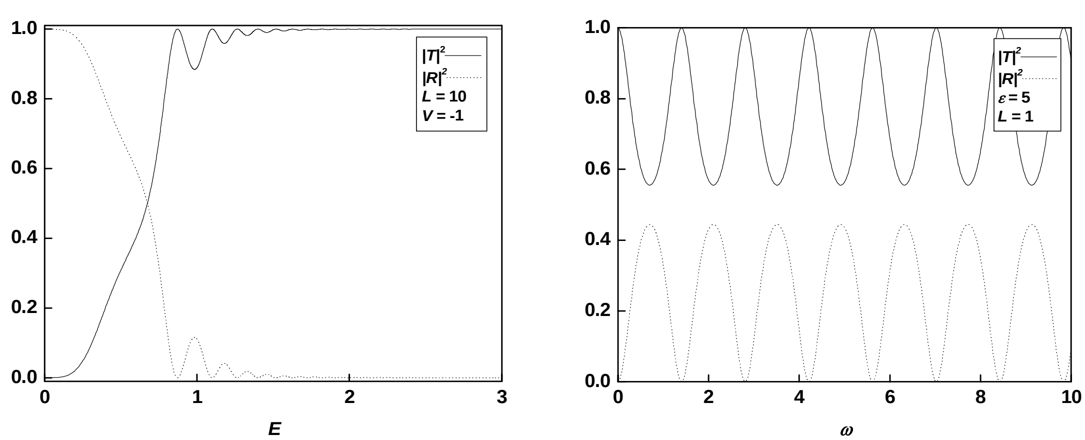

Figure 4.4: $|R|^2$ **and** $|T|^2$ **vs.** E **for the Schrödinger wave equation (left) and vs.** ω **for the EM wave equation (right).**

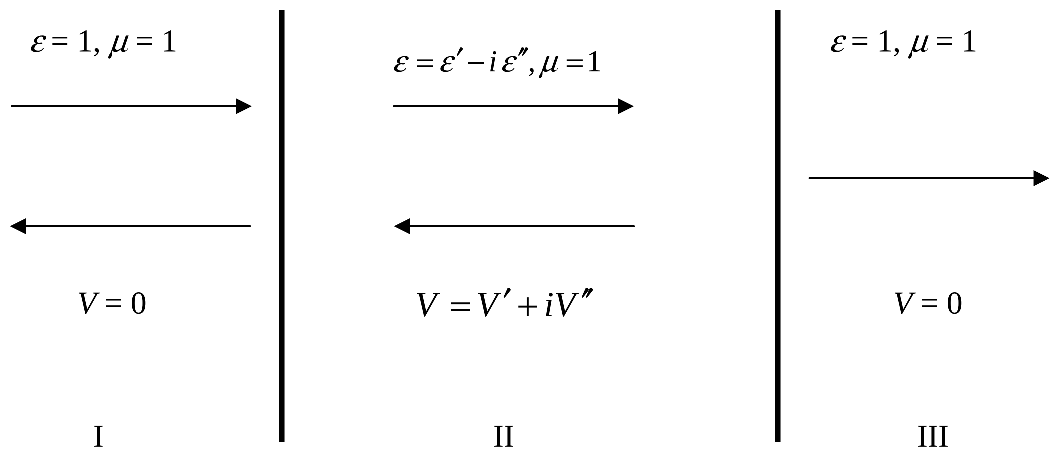

Figure 4.5: A one-dimensional scattering problem of an EM or quantum wave by a gain scattering medium of length L.

4.2. One-Dimensional Scattering Through a Gain Medium

The main task in this study is to study R and T in gain media. The potential will be of the form $V = V' + iV''$ and the permittivity will be of the form $\varepsilon = \varepsilon' - i\varepsilon''$ (V', V'', ε', ε'' are real). In the case of gain, $|R|^2 + |T|^2 > 1$ as one would expect. $|R|^2$ and $|T|^2$ for the two time-independent wave equations will be studied in parallel for comparison purposes. In all cases with gain, $\ln|R|^2$ and $\ln|T|^2$ will be plotted instead of $|R|^2$ and $|T|^2$ for convenience. First of all, $|R|^2$ and $|T|^2$ are studied vs. the gain medium length L as shown in figure 4.6. In the Schrödinger wave equation case, as shown in figure 4.6 (left), both $|R|^2$ and $|T|^2$ increase with the gain medium length, which is expected. But in contrast with physical intuition, at some critical gain medium length, which is the same for $|R|^2$ and $|T|^2$, the latter start to drop exponentially to zero after oscillating around the region of the global maxima. Conversely, the former, namely $|R|^2$, oscillates around the global maxima but saturates to some nonzero value. In the EM wave equation case, as shown in figure 4.6 (right), the behaviors of $|R|^2$ and $|T|^2$ are very similar to those in the Schrödinger wave equation case, and the critical gain medium length is again common for both $|R|^2$ and $|T|^2$. The drop in $|R|^2$ and $|T|^2$ is counter-intuitive since wave propagation should be enhanced as the wave traverses the gain medium. The dependences of $|R|^2$ and $|T|^2$ on V' in the case of the Schrödinger wave equation and on ε' in the case of the EM wave equation were studied for a gain medium and the result is depicted in figure 4.7. The figure shows very interesting behaviors for both $|R|^2$ and $|T|^2$. Moreover, it will be very illustrative to study the dependences of $|R|^2$ and $|T|^2$ on the imaginary parts of the potential V'' and permittivity ε''. This was carried out and the results are shown in figure 4.8. It is clear in the figure that both $|R|^2$ and $|T|^2$ for the two wave equations increase to a unique maximum and then start to drop exponentially at some critical values of V'' or ε''. In the case of $|T|^2$ the drop is to zero while $|R|^2$ converges to some finite value. Finally, figure 4.4 is reproduced with gain and illustrated in figure 4.9. In figure 4.9 (left), it is seen that both $|R|^2$ and $|T|^2$ are amplified in the low energy region. However, as energy increases, the incident wave becomes insensitive to the potential and its behavior becomes asymptotically similar to that in figure 4.4 (left). Nonetheless, the behaviors of $|R|^2$ and $|T|^2$ in figure 4.9 (right) are very different from those in figure 4.4 (right).

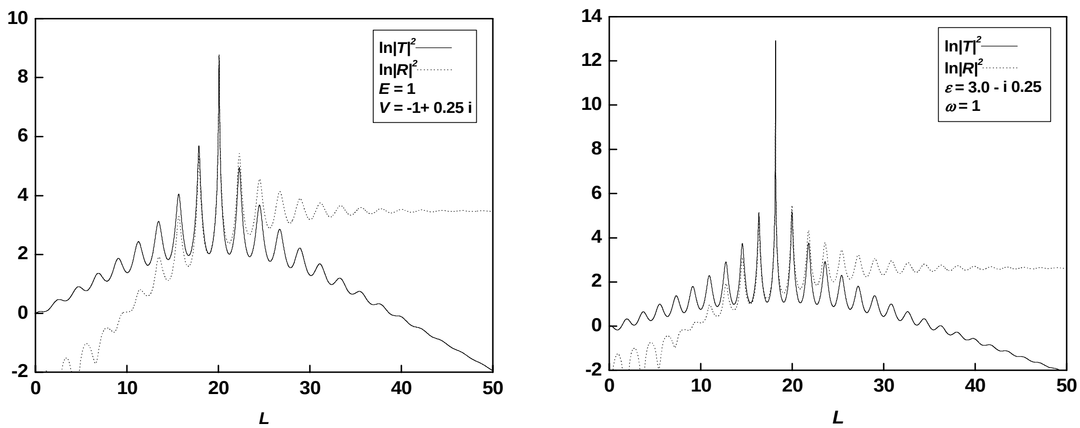

Figure 4.6: $\ln|R|^2$ and $\ln|T|^2$ vs. the gain medium length L for the Schrödinger wave equation (left) and EM wave equation (right).

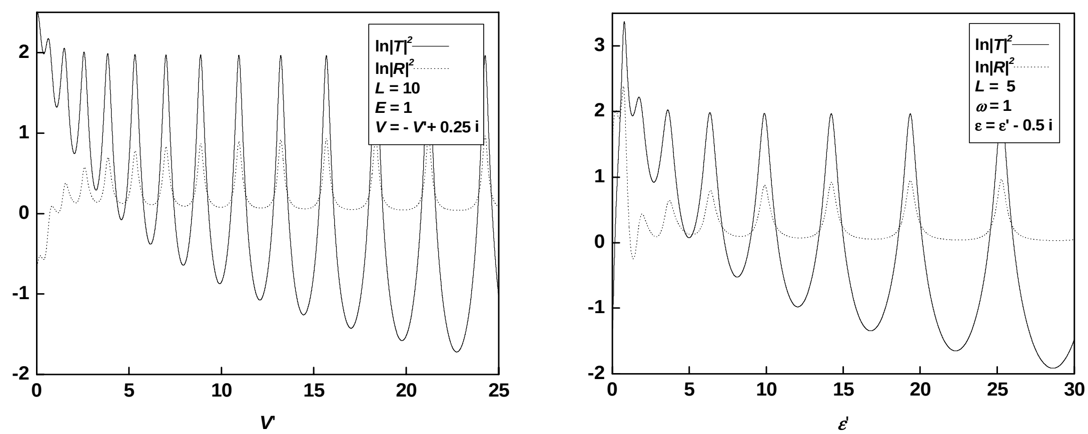

Figure 4.7: $\ln|R|^2$ and $\ln|T|^2$ with gain vs. the real potential V' for the Schrödinger wave equation (left) and vs. the real permittivity ε' for the EM wave equation (right).

It is noticeable that the similarity between the dependences of $|R|^2$ and $|T|^2$ on L and ω are evident even with gain in the case of the EM wave equation.

Of course there is a relation between the critical gain medium length and the gain intensity, the value of the imaginary part of the potential V'' or permittivity ε''. The relation was studied numerically for the two wave equations and the results are shown in figure 4.10.

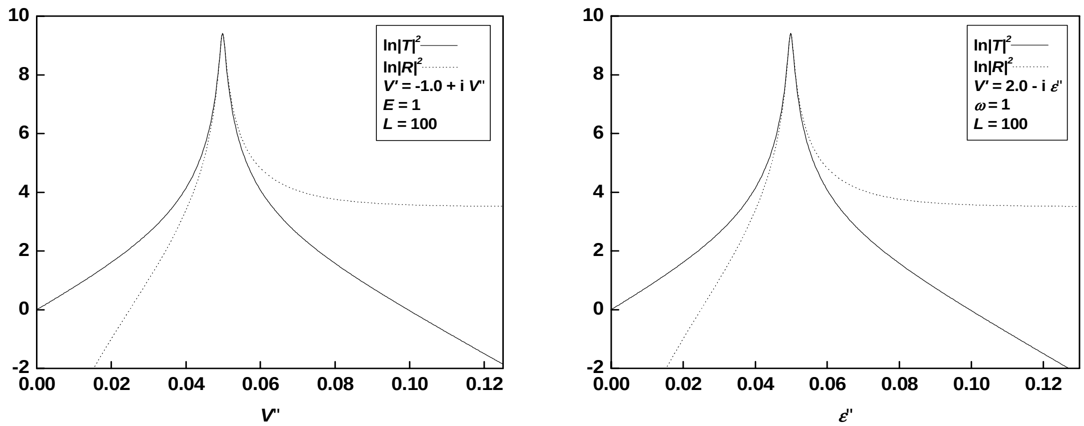

Figure 4.8: $\ln|R|^2$ **and** $\ln|T|^2$ **with gain vs. the imaginary part of the potential** V'' **for the Schrödinger wave equation (left) and vs. the imaginary part of the permittivity** ε'' **for the EM wave equation (right).**

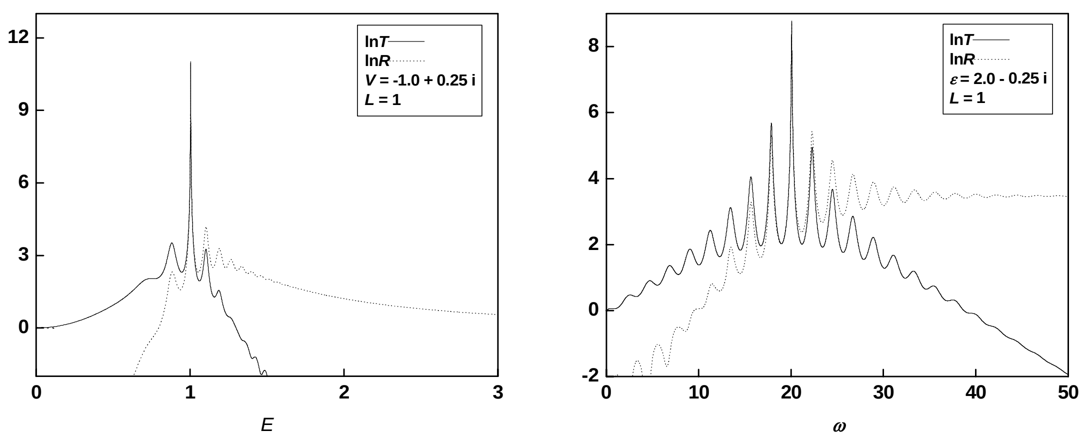

Figure 4.9: $\ln|R|^2$ **and** $\ln|T|^2$ **with gain vs.** E **for the Schrödinger wave equation (left) and vs.** ω **for the EM wave equation (right).**

The relation between $V_c''(L)$ or $\varepsilon_c''(L)$ (the critical gain intensity at some L) and L is roughly inverse proportionality.

It is important to say that fixing L and changing V'' will show only one peak, as depicted in figure 4.8. On the other hand, fixing V'' and changing L will result in several peaks as shown in figures 4.6. This issue will be clarified in chapter 5 where resonance poles are discussed.

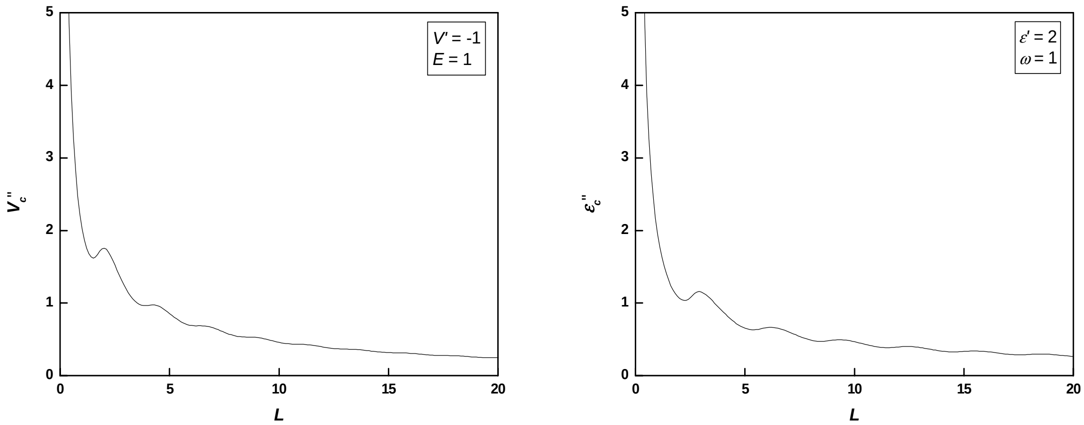

Figure 4.10: The dependence of V_c'' on *L* for the Schrödinger wave equation (left) and EM wave equation (right).

CHAPTER 5

5. RESONANCE POLES

5.1. Resonance Poles of *R* and *T* of the Time-Independent Wave Equations

The resonance poles of *R* or *T* are the points in the complex *k*-plane (or *E*-plane) in the case of the Schrödinger wave equation and in the complex ω-plane in the case of the EM wave equation, at which *R* or *T* is infinite. In chapter 4, analytical expressions were found for both *R* and *T* for the two wave equations

$$T = \frac{4e^{-iL\left(k-\sqrt{k^2-V}\right)}k\sqrt{k^2-V}}{e^{2iL\sqrt{k^2-V}}\left(k-\sqrt{k^2-V}\right)^2-\left(k+\sqrt{k^2-V}\right)^2} \tag{4.9}$$

$$R = V\frac{1-e^{2iL\sqrt{k^2-V}}}{e^{2iL\sqrt{k^2-V}}\left(k-\sqrt{k^2-V}\right)^2-\left(k+\sqrt{k^2-V}\right)^2} \tag{4.10}$$

for the Schrödinger wave equation, and

$$T = \frac{4e^{2iL\left(\sqrt{\varepsilon}-1\right)\omega}\sqrt{\varepsilon}}{e^{2iL\sqrt{\varepsilon}\omega}\left(\sqrt{\varepsilon}-1\right)^2-\left(\sqrt{\varepsilon}+1\right)^2} \tag{4.11}$$

$$R = \frac{\left(e^{2iL\sqrt{\varepsilon}\omega}-1\right)\left(\varepsilon-1\right)}{e^{2iL\sqrt{\varepsilon}\omega}\left(\sqrt{\varepsilon}-1\right)^2-\left(\sqrt{\varepsilon}+1\right)^2} \tag{4.12}$$

for the EM wave equation. Due to the fact that *R* and *T* have the same denominators, their resonance poles are identical. Equating the denominators of these equations to zero yields that the resonance poles are those that satisfy the following equations

$$\left(\frac{\sqrt{k^2 - V} + k}{\sqrt{k^2 - V} - k}\right)^2 = e^{2iL\sqrt{k^2 - V}} \tag{5.1}$$

in the Schrödinger equation case, and

$$\left(\frac{\sqrt{\varepsilon} + 1}{\sqrt{\varepsilon} - 1}\right)^2 = e^{2i\omega L\sqrt{\varepsilon}} \tag{5.2}$$

in the wave equation case. Further discussion on the resonance poles and their correlation to the behaviors of *R* and *T* will be presented in the next two subsections.

5.1.1. The Resonance Poles in a Gainless Medium

The roots (resonance poles) of equations 5.1 and 5.2 are shown in figures 5.1 and 5.2, respectively for a gainless scattering medium. The numerical approach used to locate the complex poles of Eq. 5.1 was introduced in chapter 2.

Now let us study *R* and *T* in the vicinity of the resonance poles. In figure 5.3 (left), we see that $|R|^2$ and $|T|^2$ resonate when *E* becomes very close to the real part of a resonance pole in the complex *E*-plane. The same is true for figure 5.3 (right), where $|R|^2$ and $|T|^2$ resonate when ω becomes very close to the real part of a resonance pole in the complex ω-plane. However, in all cases, $|R|^2$ is minimum when $|T|^2$ is maximum and vice versa. Generally speaking, $|R|^2$ and $|T|^2$ will be infinite if and only if a pole has *k* or ω purely real, which will never happen in gainless media. This point will be clarified below.

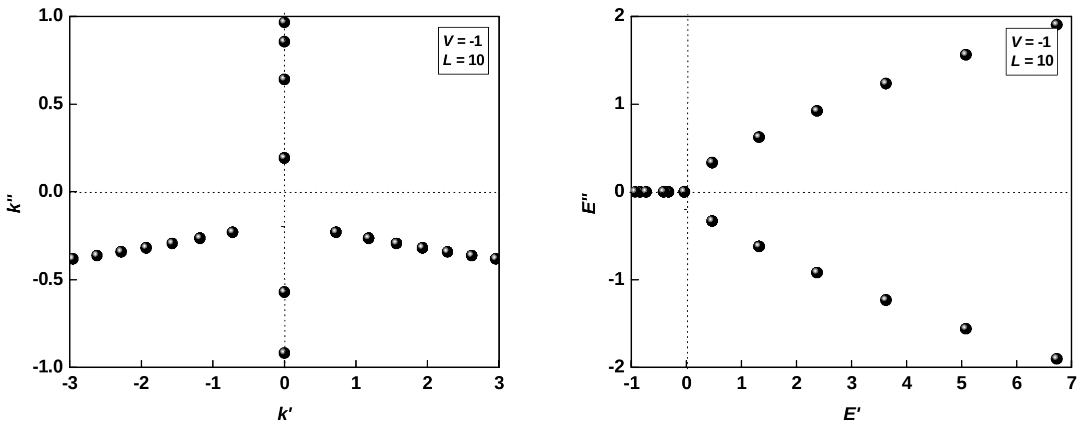

Figure 5.1: The resonance poles of *R* and *T* the Schrödinger equation in a gainless medium in the complex *k*-plane (left) and *E*-plane (right).

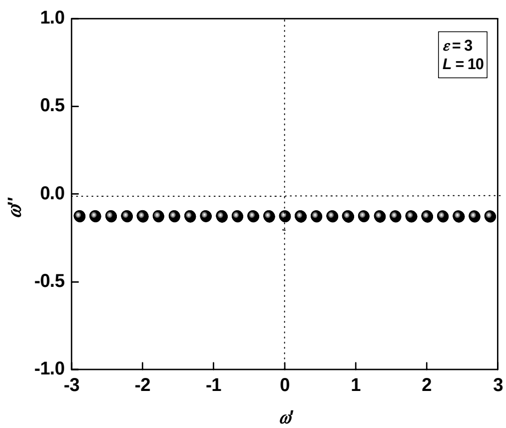

Figure 5.2: The resonance poles of *R* and *T* in a gainless medium of the EM wave equation in the complex ω-plane.

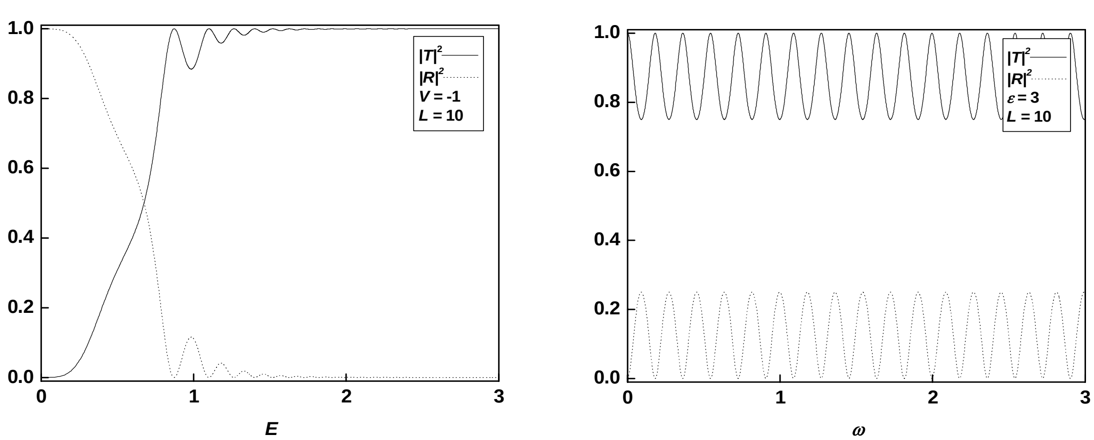

Figure 5.3: $|R|^2$ and $|T|^2$ in a gainless medium vs. E for the Schrödinger wave equation (left) and vs. ω for the EM wave equation (right).

5.1.2. The Resonance Poles in a Gain Medium

In this subsection the figures in the previous subsection will be reproduce but for gain media. The poles in a gain medium are shown in figures 5.4 and 5.5 for the Schrödinger and EM wave equations respectively. The effect of gain on the poles is very evident. The correlation between these poles and the behaviors of $|R|^2$ and $|T|^2$ slightly differs from that in the previous subsection. Even in the case of gain it is still true that both $|R|^2$ and $|T|^2$ resonate, with $|R|^2$ is minimum when $|T|^2$ is maximum and vice versa, when E or ω becomes very close to the real part of a resonance pole. However, at some critical transition values of E or ω, both $|R|^2$ and $|T|^2$ become maximum or minimum together. But it is not completely clear whether the situation will change back or not, i.e. $|R|^2$ or $|T|^2$ become maximum when the other is minimum and vice versa. The transition is illustrated in figure 5.6 where $|R|^2$ and $|T|^2$ are plotted versus E or ω for the two wave equations.

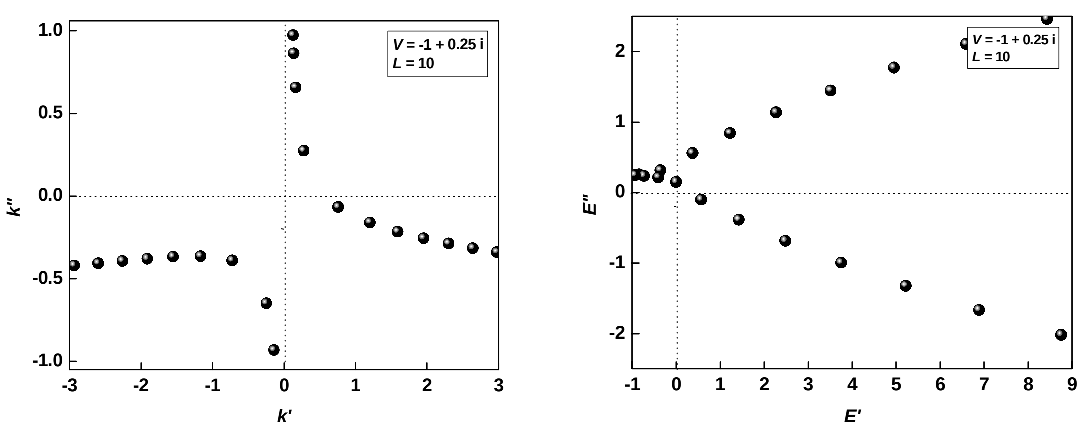

Figure 5.4: The resonance poles of *R* and *T* for the Schrödinger equation in a gain medium in the complex *k*-plane (left) and *E*-plane (right).

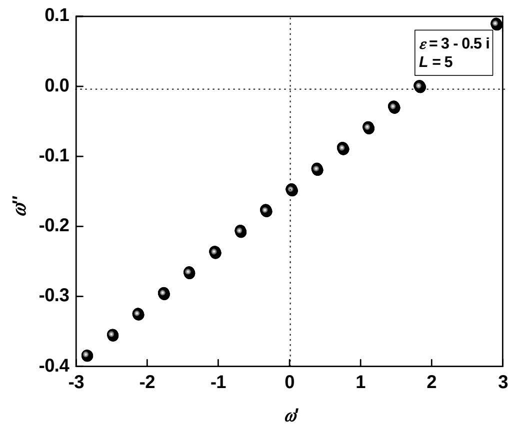

Figure 5.5: The resonance poles of *R* and *T* in a gain medium of the EM wave equation in the complex *ω*-plane.

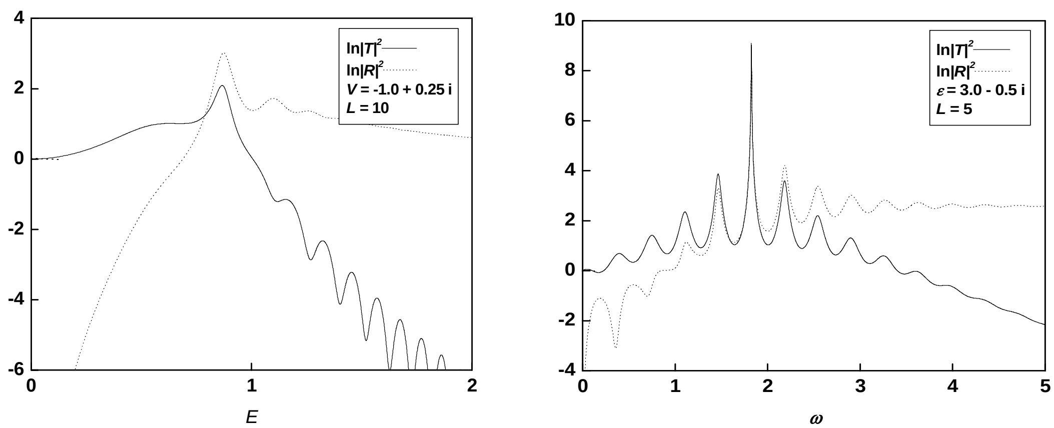

Figure 5.6: $|R|^2$ and $|T|^2$ with gain vs. E for the Schrödinger wave equation (left) and vs. ω for the EM wave equation (right).

It is worth mentioning that $|R|^2$ and $|T|^2$ will show merely a single peak when they are plotted vs. V'' or ε''. On the other hand, $|R|^2$ and $|T|^2$ will show multiple peaks with different heights when they are plotted vs. L, V' or ε', or E or ω. This fact can be clearly observed in figures 4.6, 4.7, 4.8 and 4.9. The difference between the effects of these four parameters comes from the different influences they have on the resonance poles. As V'' or ε'' change, $|R|^2$ and $|T|^2$ coincide with a resonance pole or bypass it closely, and then get away from it and never see its effect significantly. Besides, as L, V' or ε', or E or

ω changes, $|R|^2$ and $|T|^2$ coincide with a resonance pole or bypass it closely resulting in a peak, and then, as the parameters change more, $|R|^2$ and $|T|^2$ coincide with or bypass another pole closely resulting in another peak. And this process continues numerous times as these parameters change resulting in multiple peaks. It is important to mention that $|R|^2$ and $|T|^2$ may coincide exactly with a resonance pole once at most when one of the parameters is changed. In the special case where the poles are nearly aligned in a horizontal line, one would conclude that the effect of altering V'' or ε'' will be mainly to shift the poles vertically. While the effect of altering L, or V' or, ε' or ω or E would be mainly to shift, contract or dilate the poles horizontally.

5.1.3. The Resonance Poles in a Gain Medium with an Energy Dependent Potential

A linearly energy dependent potential will be of special interest to us since it serves as a link between the two wave equations as was shown in chapter 3. The replacement of V with $k^2 v$ in Eq. 4.9 and Eq. 4.10 where v is a proportionality constant, will transform them into

$$T = \frac{4e^{-iLk\left(1-\sqrt{1-v}\right)}\sqrt{1-v}}{e^{2iLk\sqrt{1-v}}\left(1-\sqrt{1-v}\right)^2 - \left(1+\sqrt{1-v}\right)^2} \tag{5.3}$$

$$R = v\frac{1-e^{2iLk\sqrt{1-v}}}{e^{2iLk\sqrt{1-v}}\left(1-\sqrt{1-v}\right)^2 - \left(1+\sqrt{1-v}\right)^2}\,. \tag{5.4}$$

Also, the poles Eq. 5.1 becomes

$$\left(\frac{\sqrt{1-v}+1}{\sqrt{1-v}-1}\right)^2 = e^{2iLk\sqrt{1-v}}. \qquad (5.5)$$

The analogy between Eq. 5.3, Eq. 5.4 and Eq. 5.5, and Eq. 4.11, Eq. 4.12 and Eq. 5.2 is unequivocal. Figure 5.7 depicts $|R|^2$ and $|T|^2$ defined by Eq. 5.3 and Eq. 5.4 in gainless and gain media. Figures 5.8 and 5.9 show the poles of Eq. 5.5 in gainless and gain media in the *k*- and *E*- complex planes, respectively.

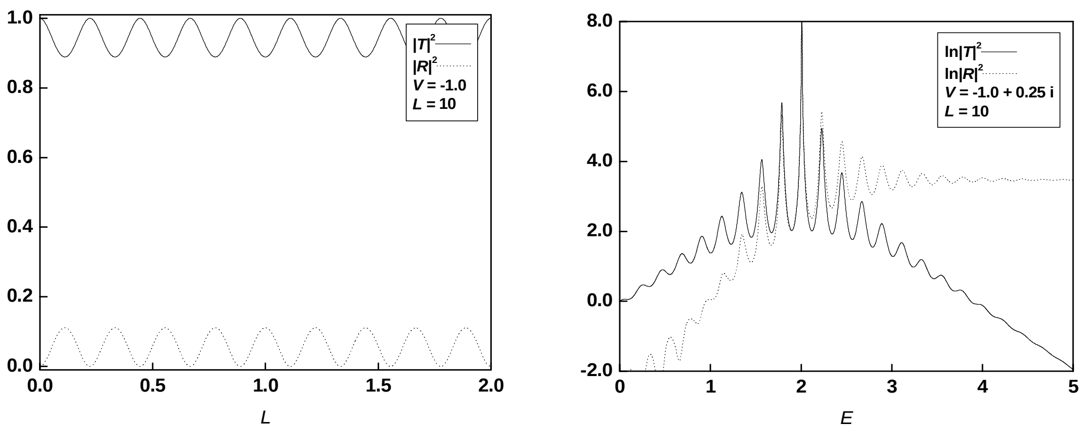

Figure 5.7: $|R|^2$ and $|T|^2$ vs. *L* with a potential directly proportional to the energy for the Schrödinger wave equation in a gainless medium (left) and gain medium (right),

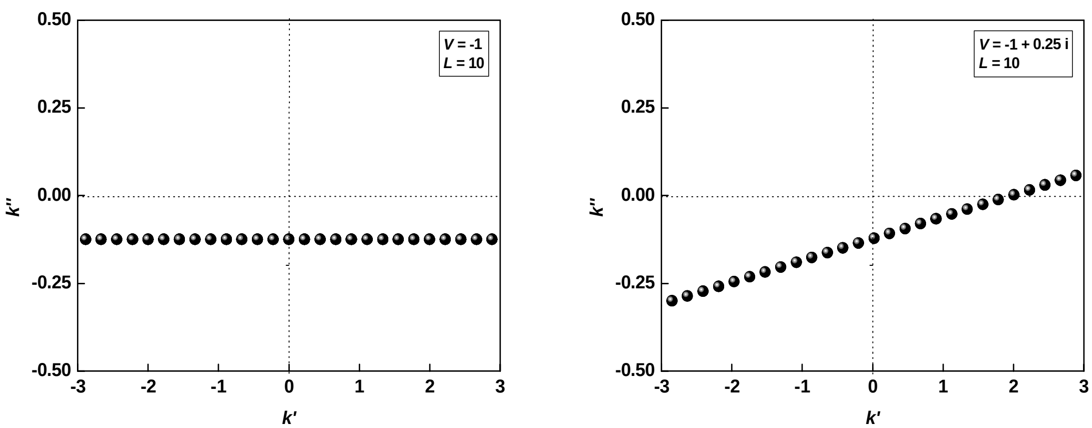

Figure 5.8: The resonance poles of *R* and *T* with a potential directly proportional to the energy for the Schrödinger wave equation in the complex *k*-plane in a gainless medium (left) and gain medium (right).

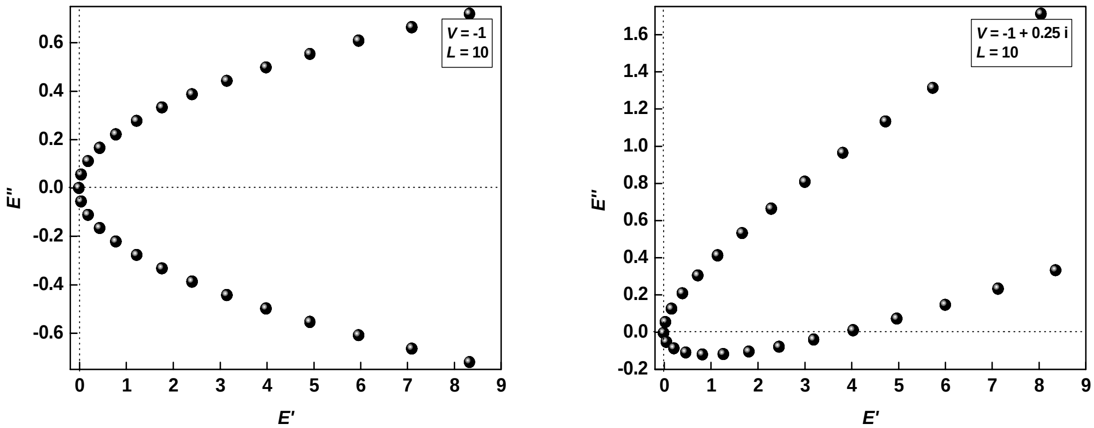

Figure 5.9: The resonance poles of *R* and *T* with a potential directly proportional to the energy for the Schrödinger wave equation in the complex *E*-plane in a gainless medium (left) and gain medium (right).

In figures 5.10 and 5.11, the poles of *R* and *T* for the Schrödinger equation with potentials with two different energy dependencies are shown. It is very evident that the best mapping between the EM and Schrödinger wave equations is obtained through using an energy dependent potential with direct proportionality.

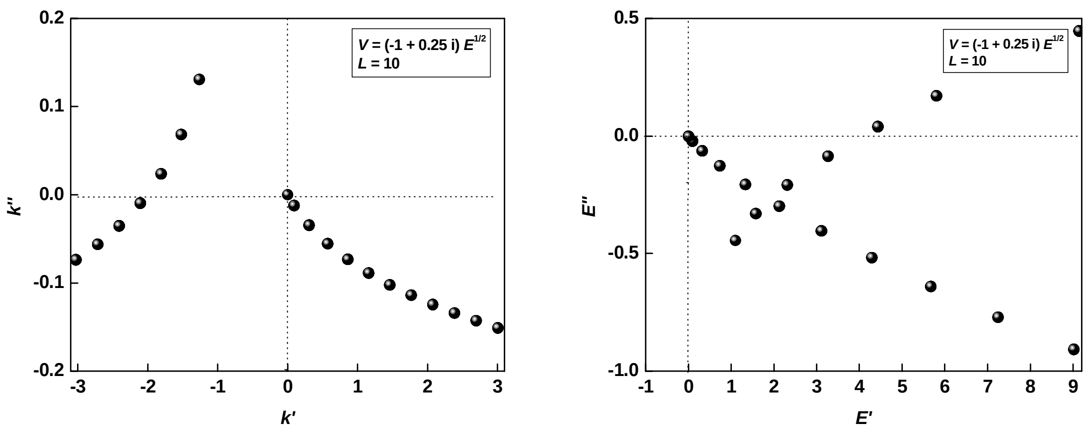

Figure 5.10: The resonance poles of *R* and *T* with a potential $V \propto \sqrt{E}$ for the Schrödinger wave equation in the complex *k*-plane (left) and *E*-plane (right).

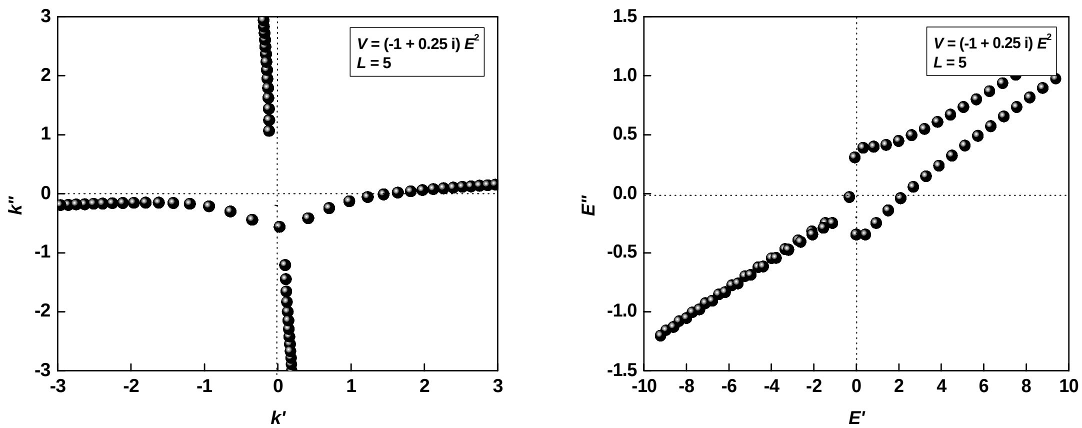

Figure 5.11: The resonance poles of *R* and *T* with a potential $V \propto E^2$ for the Schrödinger wave equation in the complex *k*-plane (left) and *E*-plane (right).

5.1. Analytical Solutions of the Poles Equations for the EM Wave Equation and the Schrödinger Wave Equation with a Potential Directly Proportional to the Energy

Because Eq. 5.2 and Eq. 5.5 are of special significance and have analytical solutions, they were studied analytically. Eq. 5.2 and Eq. 5.5 have the following analytical solutions, respectively,

$$k = \left(i\, Log\left(\frac{\sqrt{1-v}+1}{\sqrt{1-v}-1} \right) + n\pi \right) \frac{1}{L\sqrt{1-v}} \tag{5.6}$$

$$\omega = \left(i\, Log\left(\frac{\sqrt{\varepsilon}+1}{\sqrt{\varepsilon}-1} \right) + n\pi \right) \frac{1}{L\sqrt{\varepsilon}}\,. \tag{5.7}$$

With $k = k' + i\,k''$, Eq. 5.6 can be separated into real and imaginary parts. After sophisticated complex analysis, the following expressions were obtained

$$k' = \left(n\pi - \tan^{-1}\left(\frac{2r\sin\theta}{r^2-1} \right) \cos\theta - \frac{1}{2}\ln\left(2\frac{r^2+1}{r^2-2r\cos\theta+1} - 1 \right) \sin\theta \right) \frac{1}{Lr} \tag{5.8}$$

$$k'' = \left(n\pi + \tan^{-1}\left(\frac{2r\sin\theta}{r^2 - 1} \right)\sin\theta + \frac{1}{2}\ln\left(2\frac{r^2+1}{r^2 - 2r\cos\theta + 1} - 1 \right)\cos\theta \right)\frac{-1}{Lr} \qquad (5.9)$$

where

$$\theta = \frac{1}{2}\tan^{-1}\frac{v''}{v'-1} \qquad (5.10)$$

and

$$r = ((v'-1)^2 + v''^2)^{1/4}. \qquad (5.11)$$

A similar treatment for equation 5.7 yielded,

$$\omega' = \left(n\pi - \tan^{-1}\left(\frac{2r\sin\theta}{r^2 - 1} \right)\cos\theta - \frac{1}{2}\ln\left(2\frac{r^2+1}{r^2 - 2r\cos\theta + 1} - 1 \right)\sin\theta \right)\frac{1}{Lr} \qquad (5.12)$$

$$\omega'' = \left(n\pi + \tan^{-1}\left(\frac{2r\sin\theta}{r^2 - 1} \right)\sin\theta + \frac{1}{2}\ln\left(2\frac{r^2+1}{r^2 - 2r\cos\theta + 1} - 1 \right)\cos\theta \right)\frac{-1}{Lr} \qquad (5.13)$$

where

$$\theta = \frac{1}{2}\tan^{-1}\frac{\varepsilon''}{\varepsilon'} \qquad (5.14)$$

and

$$r = (\varepsilon'^2 + \varepsilon''^2)^{1/4}. \qquad (5.15)$$

With these relations, it will be straightforward to study the influence of each parameter on the poles.

CHAPTER 6

6. TIME-DEPENDENT WAVE EQUATIONS

Due to the unphysical results obtained from the time-independent wave equations, one has to look at the same problem from another point of view, namely, the time-dependent wave equations. The problem in Chapter 4 that is illustrated in figures 4.1 and 4.5 was tackled from the time-dependent approach. The time-dependent Schrödinger and EM wave equations were solved numerically using the Finite Difference method. The details of the numerical solutions were offered in chapter 2. As mentioned in chapter 2, the reflection and transmission coefficients for the Schrödinger wave equations are given respectively by [21]

$$|R(t)|^2 = \int_{-\infty}^{x_i} |\xi(x,t)|^2 \, dx \tag{2.43}$$

$$|T(t)|^2 = \int_{x_f}^{\infty} |\xi(x,t)|^2 \, dx \tag{2.44}$$

The incident wave in the Schrödinger equation case is a Gaussian wave packet with an average momentum k_0 and a variance of σ i.e.

$$\psi(x,0) = e^{-\frac{(x-x_0)^2}{2\sigma^2}} e^{i x k_0} . \tag{2.42}$$

In the EM wave equation case, the initial wave could be a plane wave or a Gaussian pulse. However monochromatic waves are more suitable since they are easier to handle than multichromatic pulses, and moreover, we are interested resonance effects. Plane wave are approximated using the waveform

$$f(x) = \frac{e^{i\omega_0 x}}{1 + e^{\frac{(x-x_0)^2}{a^2} - b^2}} \tag{2.45}$$

which yields a near exact representation for large a.

6.1. One-Dimensional Scattering Through a Gainless Medium

The transmission and reflection coefficients were calculated numerically for the two time-dependent wave equations as function of time. A Gaussian wave packet was used as an initial input for the Schrödinger wave equation while the modified plane wave (see chapter 2) was used in the case of the EM wave equation. In figure 6.1 the scattering medium is very small relative to the incident waves widths. The results are reproduced and shown for media with more intense scattering in figure 6.2. Moreover, $|R|^2 + |T|^2$ is shown as well in the first three figures of this chapter. In figure 6.1 it is evident that $|R|^2$ and $|T|^2$ add to 1 before and after the scattering occurs. The drop in $|R|^2 + |T|^2$ is due to the fact that a part of the incident waves resides inside the scattering medium for a while. This effect is also clear in the case of strong scattering for the two wave equations, as shown in figure 6.2. Recalculating $|R|^2$ and $|T|^2$ for a scattering medium whose length is close to the wave effective incident waves widths (roughly the width at hundredth maximum in the case of Gaussian wave packets) will illuminate the interesting result of the two previous figures as demonstrated in figure 6.3.

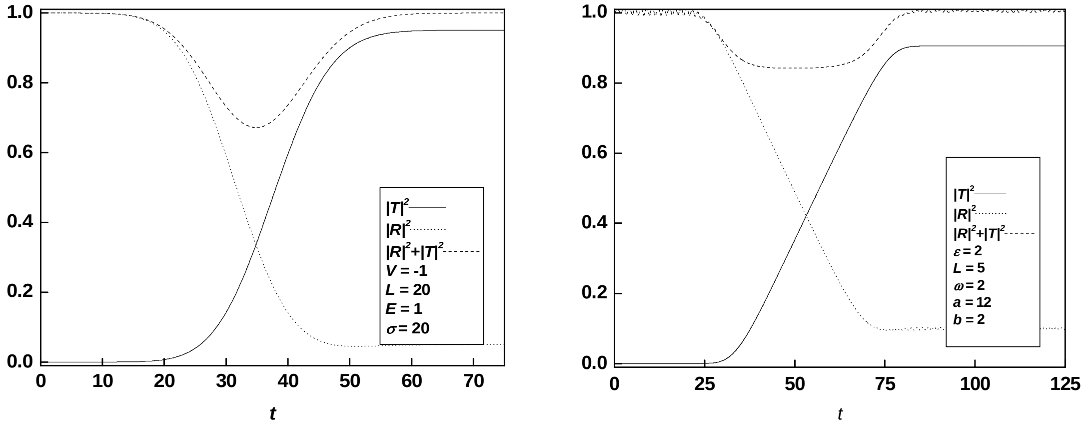

Figure 6.1: $|T|^2$ **and** $|R|^2$ **vs. time for a small gainless medium for the Schrödinger wave equation (left) and EM wave equation (right).**

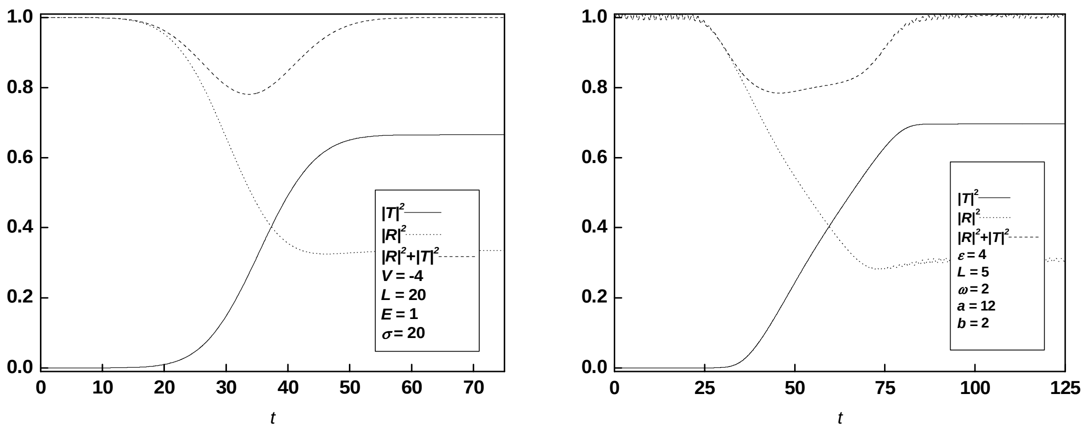

Figure 6.2: $|T|^2$ **and** $|R|^2$ **vs. time for a small gainless medium with strong scattering for the Schrödinger wave equation (left) and EM wave equation (right).**

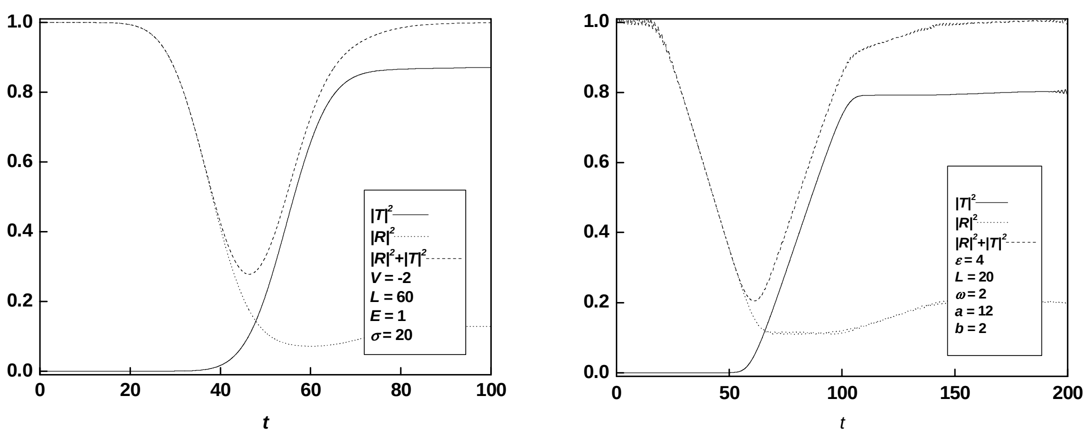

Figure 6.3: $|T|^2$ **and** $|R|^2$ **vs. time for a small gainless medium with strong scattering for the Schrödinger wave equation (left) and EM wave equation (right).**

In that case, $|R|^2$ and $|T|^2$ do not add to 1 for the two wave equations most of the time. This is similar to what happened in the last two figures above where a part of the incident wave remains in the scattering medium temporarily. It will be seen in the coming sections that this temporarily resident part of the incident wave will play a major role in gain media.

6.2. One-Dimensional Scattering Through a Gain Medium

To make parallelism between this chapter and chapter 4, the scattering through a gain medium should be tackled from a time-dependent approach as well, which is one of the main purposes of this work. The figures in the previous section were reproduced for a gain medium. Figure 6.4 shows that the effect of gain on a small medium relative to the incident wave width is to amplify the reflected and transmitted waves smoothly. Moreover, in a medium whose length is roughly close to the wave width the effect of gain is to amplify the reflected and transmitted waves in a step like process as illustrated in figures 6.5 and 6.6. In all cases, after some time, $|R|^2$ and $|T|^2$ will have nearly the same magnitude, but they will remain out of phase as can be seen in figures 6.5 and 6.6. The presence of gain in a scattering medium may make it act as an everlasting wave source, as in the case of figure 6.6.

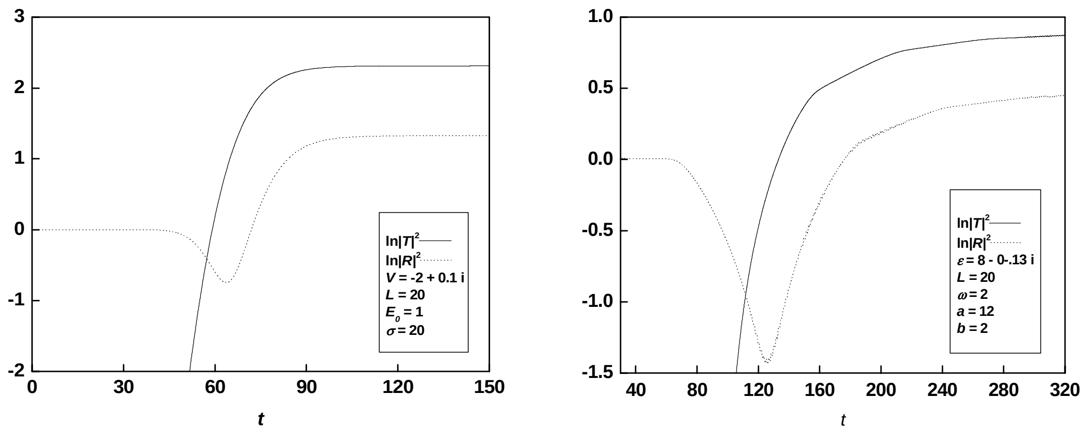

Figure 6.4: $\ln|T|^2$ **and** $\ln|R|^2$ **vs. time for a small gain medium for the Schrödinger wave equation (left) the EM wave equation (right).**

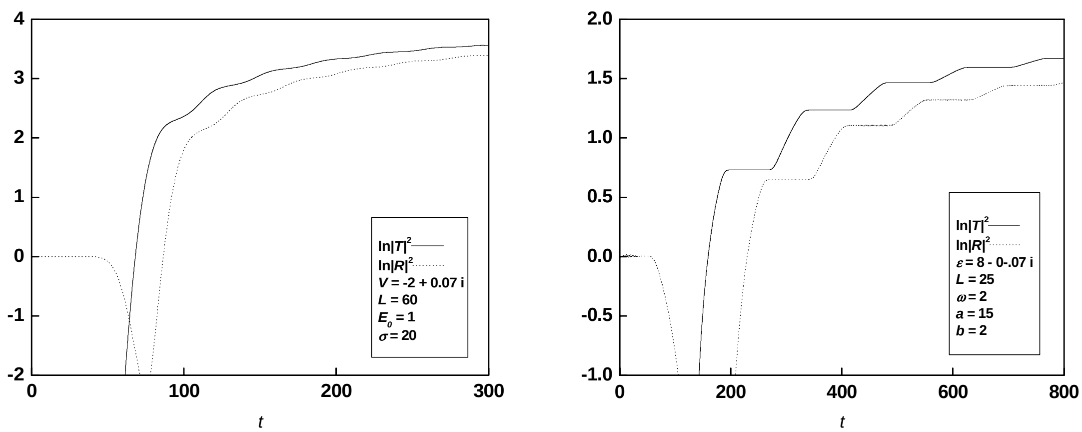

Figure 6.5: $\ln|T|^2$ **and** $\ln|R|^2$ **vs. time for a large size gain medium for the Schrödinger wave equation (left) the EM wave equation (right).**

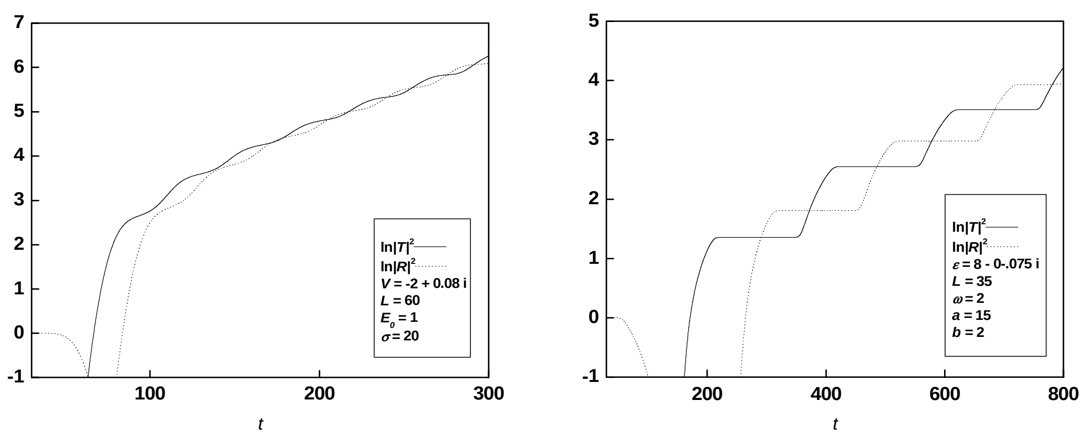

Figure 6.6: $\ln|T|^2$ **and** $\ln|R|^2$ **vs. time for a large size gain medium with high gain for the Schrödinger wave equation (left) the EM wave equation (right).**

This will be the case unless the gain medium is below some critical gain value or the gain medium size is smaller than a critical size (the two parameters are dependent), as in the case of figures 6.4 and 6.5 where $|R|^2$ and $|T|^2$ saturate to some finite values. The behavior of the transmitted wave in the case of gain for the two wave equations is very different from that specified by the time-independent wave equations. The transmission coefficient is finite below some critical gain medium length or critical gain intensity. Beyond that critical gain medium length or critical gain intensity, the transmission and reflection coefficients increase exponentially with no bound with time. This is because the wave trapped inside the gain medium gets continuously amplified by more than what it loses through leakage at the gain medium ends as reflections or transmissions. Of course these results are more physical and realistic than those given by the time-independent wave equations. The gain in fact enhances wave propagation but does not suppress it. This conclusion was previously stated in the literature by Soukoulis et al for the EM wave equation [2] and the Schrödinger wave equation [3] as well. Unfortunately, no satisfactory explanation for the discrepancy between the time-independent and time-dependent approaches was available prior to our work [1].

6.3. Waves Inside a Gain Medium

To show clearly the mechanism in which waves are being amplified in gain media, it is instructive to study the behavior of the waves inside the gain medium as function of time. In figures 6.7, 6.8 and 6.9, the wave inside the gain medium is shown vs. time for the Schrödinger and EM wave equation.

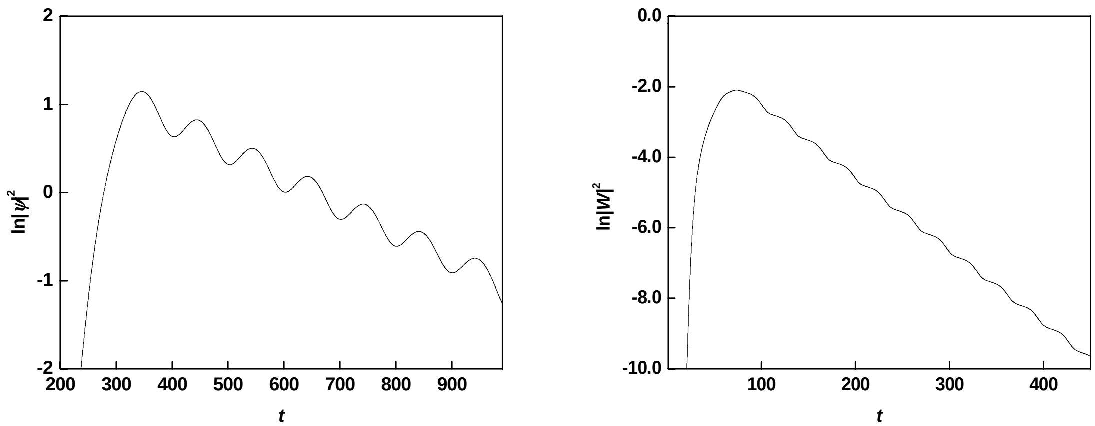

Figure 6.7: wave behavior inside a gain medium for an undercritical system for the Schrödinger wave equation (left) and the EM wave equation (right).

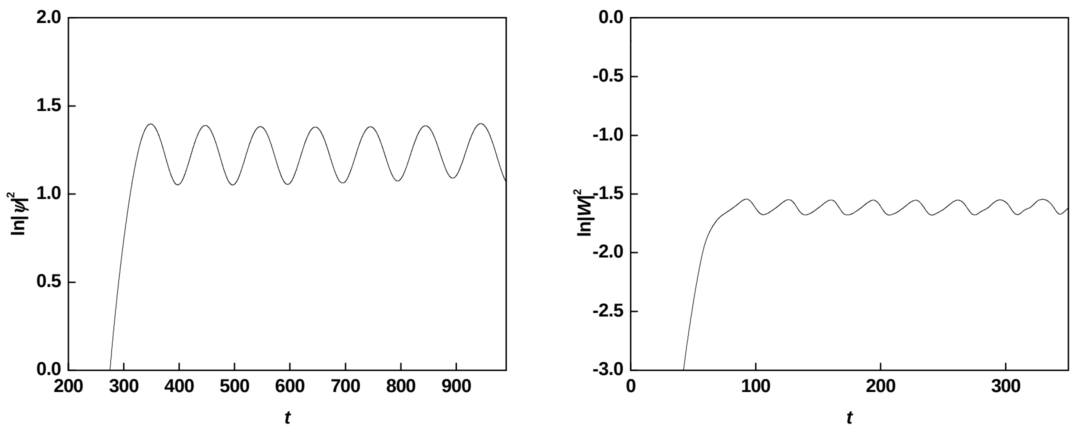

Figure 6.8: wave behavior inside a gain medium for a critical system for the Schrödinger wave equation (left) and the EM wave equation (right).

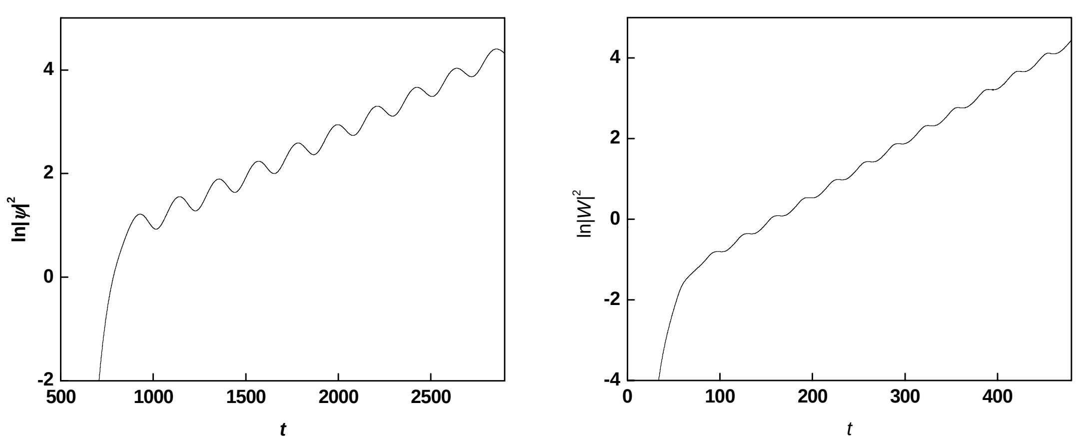

Figure 6.9: wave behavior inside a gain medium for an overcritical system for the Schrödinger wave equation (left) and the EM wave equation (right).

The three main scenarios of the waves in the gain medium can be clearly seen. When the system is undercritical, the wave enters the gain medium and gets amplified but the amplification is too feeble to compensate for the outflow from the gain medium as seen in figure 6.7. In figure 6.8 where the system is critical, the wave entered the gain medium is being amplified exactly by the same amount it loses through the outflow. Finally, figure 6.9 shows an overcritical system in which the amplification conquers the outflow and the wave inside the gain medium keeps building up.

6.4. The Multiple Reflection Approach

Since it is not trivial to solve the time-dependent wave equations analytically for R and T for the system described in chapter 4, it will be very interesting to find an alternative approach to tackle this problem. The effect of the imaginary part of the potential or permittivity will be mainly amplification while the wave is inside the gain medium as well as scattering at the boundaries of the gain medium. However, the scattering will be dominated by the real part of the potential or permittivity when the imaginary part is small relative to the real part, which is the case in our problem. Therefore, to a very good approximation, the effects of the real and imaginary parts of the potential or permittivity can be decoupled: the imaginary part will result in amplification inside the gain medium and the real part will result in scattering at the two ends of the gain medium as well as a phase shift. For an incident wave from the left, part of it will be reflected by the left end of the medium and the rest will enter it. Let the reflectance and transmittance at the left end of the gain medium be R_1 and T_1, respectively. The transmitted wave into the system will be amplified by a factor of e^{aL} where a is a real constant. Of course the transmitted wave will experience a phase shift of $e^{i\tau}$ where τ is the time it takes the wave to cross the system. This scenario is shown in figure 6.10.

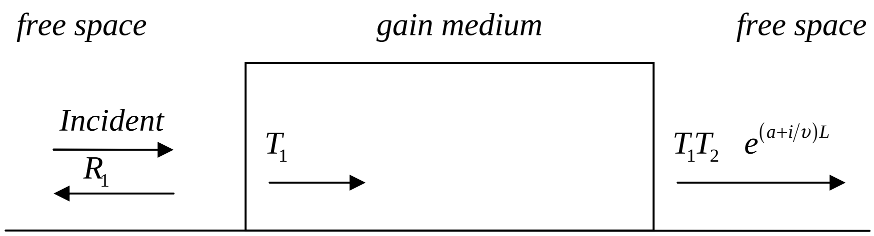

Figure 6.10: Reflection and transmission at the ends of the gain system.

τ can be written as L/υ where υ is the speed of the wave inside the gain medium. Let the reflectance and transmittance at the right end of the gain medium be R_2 and T_2, respectively. Generally, R_1 and T_1 are, respectively, the reflectance and transmittance for a wave entering the gain medium and R_2 and T_2 are the reflectance and transmittance for a wave leaving the gain medium. At the right end of the gain medium, part of the wave will be transmitted and the rest will be reflected back. The first transmitted wave will be $T_1T_2 e^{(a+i/\upsilon)L}$ as illustrated in figure 6.10. The wave reflected back to the gain medium will grow again by e^{aL} and experience a phase shift of $e^{iL/\upsilon}$ again. Then, part of it will get reflected back to the gain medium by the left end of the gain medium, grow by e^{aL} and accumulate a phase shift of $e^{iL/\upsilon}$. Again, part of it will be transmitted through the right end of the gain medium and the rest will be reflected back to gain medium. Therefore, the second transmitted wave will be $T_1 T_2 R_2^2 e^{3(a+i/\upsilon)L}$. The same process will happen again and again, as demonstrated in figure 6.11.

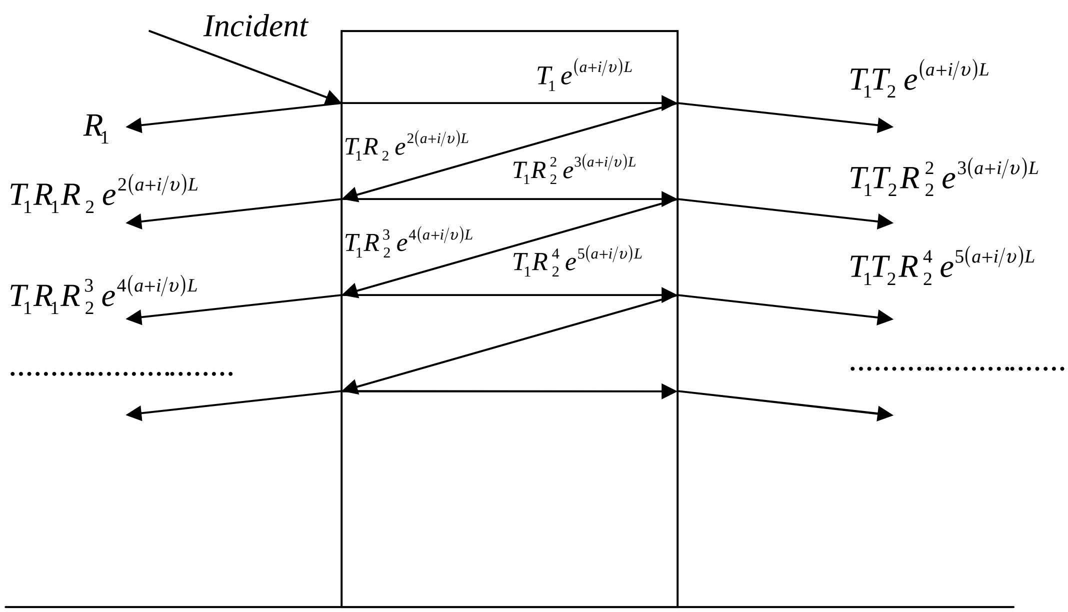

Figure 6.11: The multiple reflection events inside the scattering gain medium.

The transmission coefficient after all will be given by summing up all partial transmitted waves

$$|T|^2 = \left|T_1 T_2 \quad e^{(a+i/\upsilon)L}\right|^2 \sum_{n=0}^{\infty} \left|e^{2n(a+i/\upsilon)L} R_2^{2n}\right|^2 . \tag{6.1}$$

Of course we can express Eq. 6.1 in terms of time instead of the index n using

$$n = \frac{1}{2}\left(\frac{t}{\tau} - 1\right). \tag{6.2}$$

For the series in Eq. 6.1 to be convergent, the following condition must be satisfied

$$\left| e^{(a+i/\upsilon)L} R_2 \right| < 1 . \tag{6.3}$$

The critical value of a can be expressed as a function of L by setting the left hand side of Eq. 6.3 equal to 1 and solving for a. Doing this leads to the following expression for the critical gain intensity

$$a = \frac{i\,L - \upsilon \ln R_2}{L\,\upsilon}\,. \tag{6.4}$$

Figures 6.12, 6.13 and 6.14 are plots of $\ln|T|^2$ of Eq. 6.1 for three main values of a vs. n (or time), the summation index. In figures 6.12, 6.13 and 6.14, a is undercritical, critical and overcritical respectively. It is clear that when the system is undercritical, waiting for longer time (or adding more terms in the summation) has no effect on the output. However, the output keeps building up as time elapses (or more terms are added) when the system is overcritical.

Comparison between the numerical solutions of the time-dependent wave equations and the multiple reflections approach reveals that this approach may be applied in a more rigorous way to get an analytical solution to the time-dependent scattering problem in gain media.

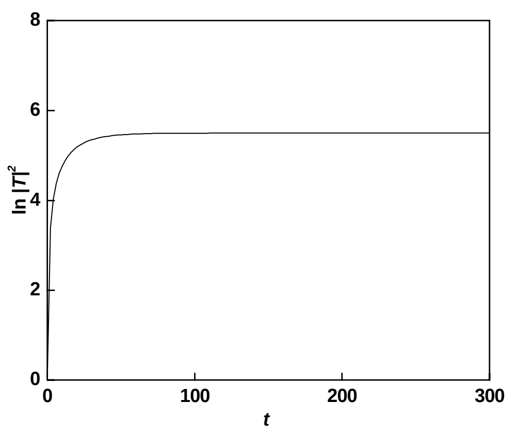

Figure 6.12: $\ln|T|^2$ **vs. time obtained from the multiple reflections approach for undercritical gain.**

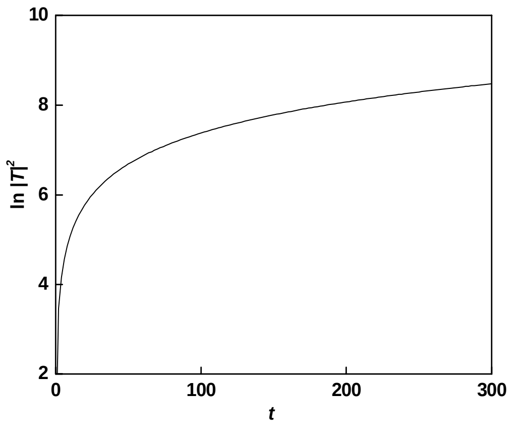

Figure 6.13: $\ln|T|^2$ **vs. time obtained from the multiple reflections approach for critical gain.**

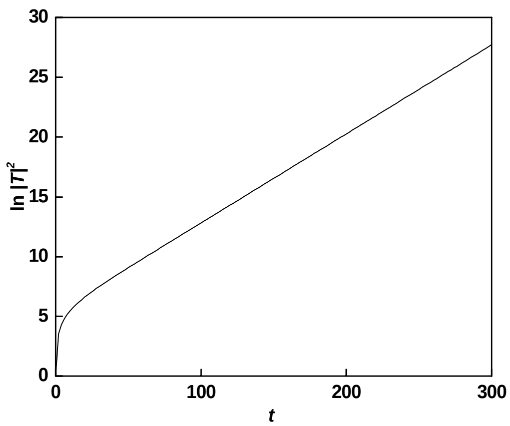

Figure 6.14: $\ln|T|^2$ **vs. time obtained from the multiple reflection approach for overcritical gain.**

6.5. Resonance Poles and the Discrepancy Between the Time-Independent and Time-Dependent Approaches

It is the main purpose of this research to try to clarify the origin of the discrepancy between the time-dependent and time-independent wave equations results in gain media. For the sake of comparison, we assert that we should study the Schrödinger wave equation with the energy dependent potential with direct proportionality ($V = vE$, where

v is a proportionality constant) in order to coherently compare it with the corresponding EM wave equation. This form of potential will make it possible to study the resonance poles analytically, exactly like in the case of the EM wave equation. As what was introduced in chapter 1, the approach used here simply relates the origin of instability and divergence in the cases of both the Schrödinger and EM wave equations to the time-dependence factors $e^{-\mathrm{i}Et/\hbar}$ and $e^{-\mathrm{i}\omega t}$, respectively. It implies that if any of the eigenstates of the systems becomes unstable and blows up then this will originate from the fact that the corresponding eigenenergy or eigenfrequency is in close proximity to one of the system resonance poles whose imaginary part is very small. Thus the structure of the resonance poles of the transmission in the complex *E*- or *ω*-plane will be studied. The value of the gain (v'' and ε'') will be tuned till one of the energy eigenvalues in the lower half of the complex energy plane approaches the real energy axis and cross it to the upper half. It is proposed in this work that this cross-over at the critical value of the gain is the origin of the discrepancy between the stationary and time-dependent behaviors.

To support the theory stated above we have to do some numerical verifications. For a gain medium with all parameters stated, we want to consider a resonance pole of interest and keep an eye on it as the imaginary part of the potential v'' or permittivity ε'' is adjusted. The moment of interest is when the pole crosses the real axis in the complex *k*- or ω -plane. Then, we want to study the time-independent transmission vs. the imaginary potential v'' or permittivity ε'' and the time-dependent transmission vs. time for different values of the imaginary part of the potential v'' or permittivity ε'' corresponding to the pole before, at and after crossing the real axis in the complex planes. In figure 6.15 (or figure 6.16) and figure 6.16 a pole under scope is traced as v'' and ε'' are adjusted in the cases of the Schrödinger and EM wave equations, respectively. Then, in figures 6.18 and 6.19, the stationary $\ln|T|^2$ is plotted vs. v'' for the Schrödinger wave equation and vs. ε'' for the EM wave equation, respectively. It is very apparent that $\ln|T|^2$ experiences a colossally sharp peak at v''_c or ε''_c (v''_c and ε''_c are the critical parameters at which a pole of interest crosses the real axis) for the two time-independent wave equations. These results are not at all astonishing since the parameters were chosen to make the denominator of the expression for transmittance vanish. The real test will be the time-dependent wave equations results. $\ln|T|^2$ was obtained by solving the time-dependent wave equations numerically for various values of v'' and ε'', below, at and above v''_c and ε''_c respectively. The results are shown for the Schrödinger wave equation in figure 6.20 and for the EM wave equation in figure 6.21. Since σ^2 is large, the approximation $V = v\,E \simeq v\,E_0$ was used, where E_0 is the average energy of the wave packet. This approximation was found numerically to be very well. The results in these two figures are, with no doubt, very supporting to the theoretical formulation even for skeptics.

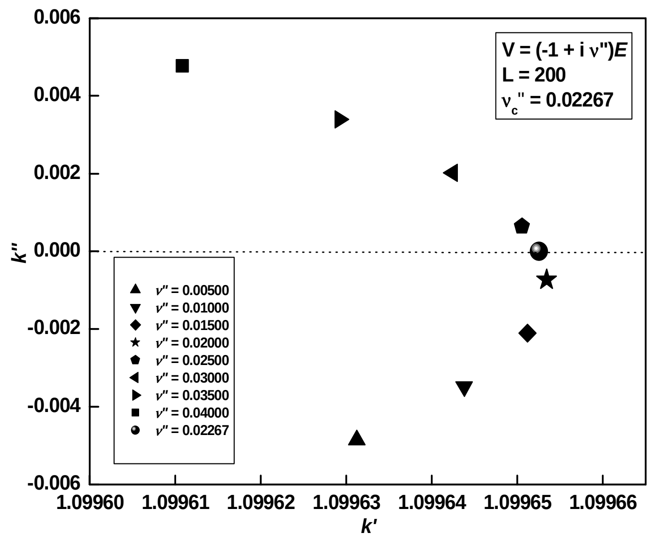

Figure 1.15: The resonance pole location in the complex *k* -plane. As *ν"* increases, the pole crosses the real axis when $\nu'' = \nu''_c = 0.02267$.

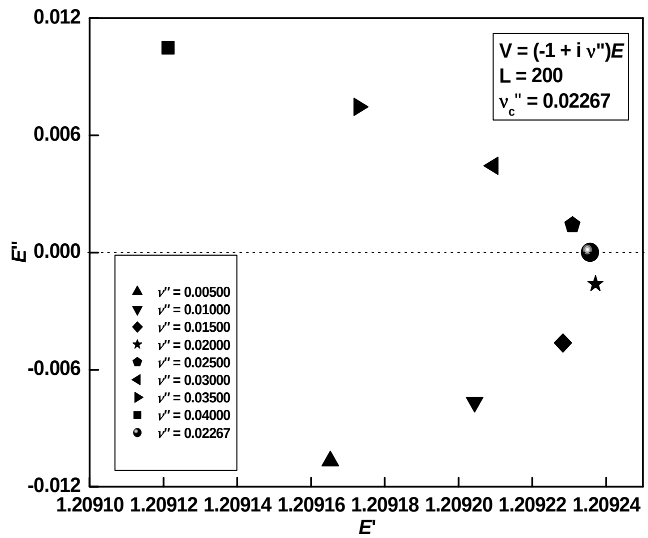

Figure 6.16: The resonance pole location in the complex *E* -plane. As ν'' increases, the pole crosses the real axis when $\nu'' = \nu''_c = 0.02267$.

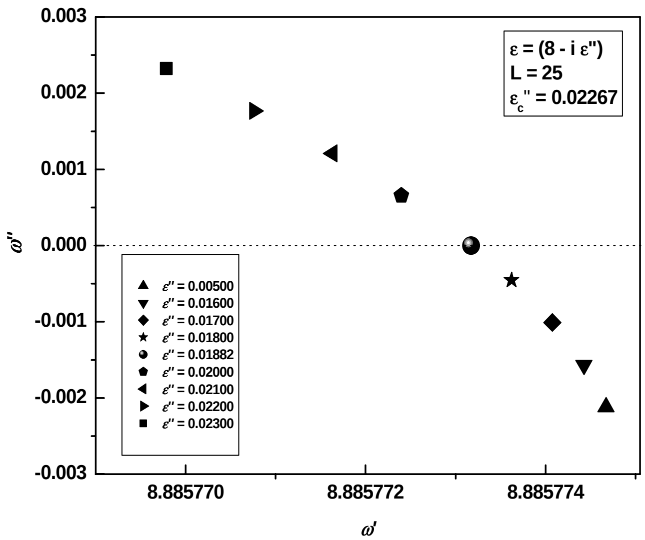

Figure 6.17: The resonance pole location in the complex ω -plane. As ε'' increases, the pole crosses the real axis when $\varepsilon'' = \varepsilon''_c = 0.01882$.

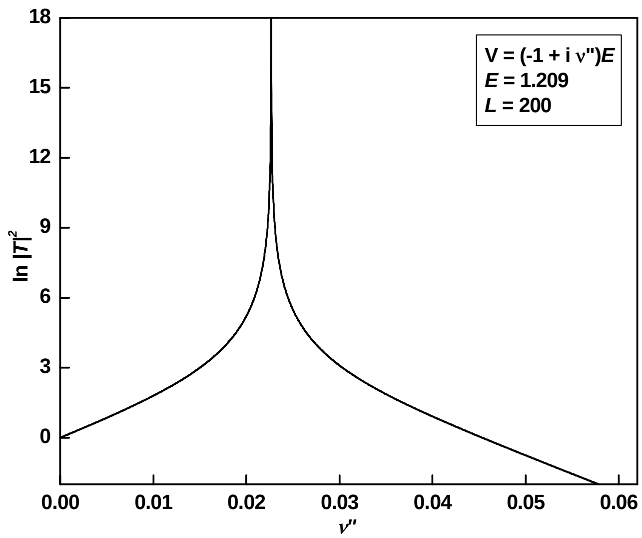

Figure 6.18: $\ln|T|^2$ obtained from the time-independent Schrödinger wave equation vs. v''. The figure shows an extremely sharp peak at $v'' = v''_c = 0.02267$.

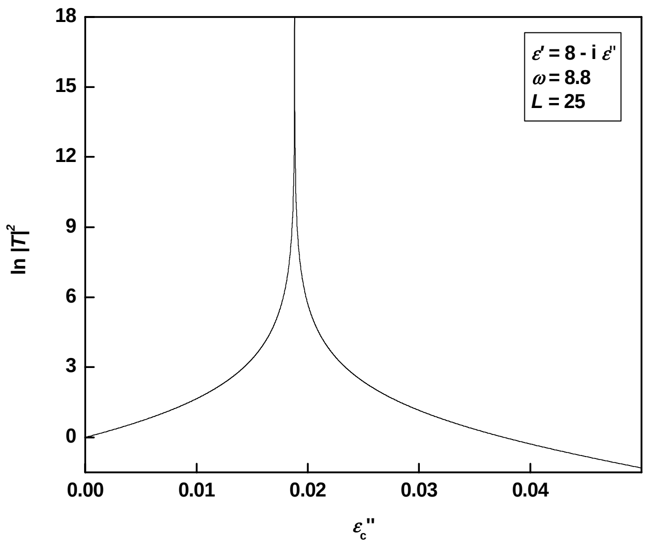

Figure 6.19: $\ln|T|^2$ **obtained from the time-independent EM wave equation vs.** ε''**. The figure shows an extremely sharp peak at** $\varepsilon'' = \varepsilon''_c = 0.01882$**.**

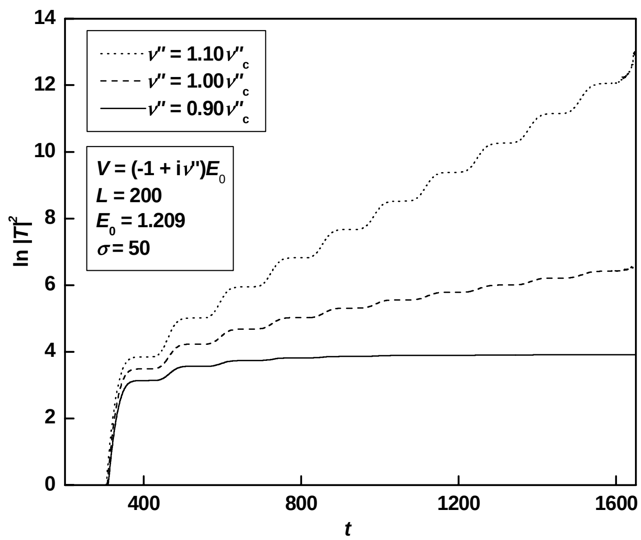

Figure 6.20: $\ln|T|^2$ **obtained from the time-dependent Schrödinger equation for three different main values of** v'' **vs. time. The figure shows clearly that the system is critical when** $v'' = v''_c = 0.02267$**.**

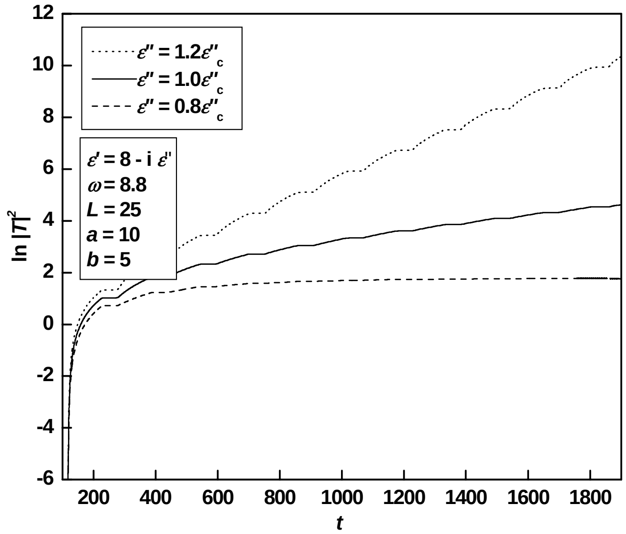

Fig. 6.21: $\ln|T|^2$ **obtained from the time-dependent EM equation vs.** ε'' **for three different values of** ε'' **vs. time. The figure shows clearly that the system is critical when** $\varepsilon'' = \varepsilon''_c = 0.01882$**.**

CHAPTER 7

7. CONCLUSION

Numerical studies proved that there is a fake dual symmetry between amplification and absorption when the problem is studied using the time-independent wave equations. After some critical gain medium length or gain intensity, the wave propagation is suppressed as if it were in a loss medium. This symmetry was refuted by the time-dependent wave equations results and shown to be merely a mathematical artifact in accordance to the work in the literature. When the gain system is critical, the reduction of time-dependant wave equations to the time-independent versions is not legitimate anymore as the stationary states are destroyed.

The parallelism in studying the Schrödinger and EM wave equations led to a mathematical mapping between the quantum waves of massive particles and the electromagnetic waves. The mapping is obtained through the use of a linearly energy dependent potential in the Schrödinger wave equation.

In order to investigate the origin of the discrepancy between the time-independent and time-dependent wave equations, the resonance poles of the reflectance and transmittance for the time-independent wave equations were studied. It was found that reflectance and transmittance have common resonance poles. As a support for the mapping between the two wave equations, it was found that the Schrödinger and EM wave equations will have similar resonance poles structures on the momentum and frequency complex planes, respectively, only if a potential directly proportional to the energy is used in the Schrödinger wave equation.

It was argued that the discrepancy between the time-independent and time-dependent wave equations originates from the time-dependence factors. As the pole that corresponds to an eigenenergy or eigenfrequency crosses the lower half plane to the upper half plane, the time-dependence factors grow with time exponentially with no bound and the stationary states are destroyed. The argument was proven numerically for the two wave equations. The transmittance for the time-independent wave equations was found to drop exponentially after the pole corresponding to the eigenenergy or eigenfrequency crosses the lower half plane to the upper half plane, after it experience a sharp peak at the crossing event. It was also found that a gain medium is critical when the corresponding pole crosses the real axis. It is undercritical before the crossing and overcritical after the crossing.

In overcritical systems where amplification plays an important role it is expected that non-linearity effect will be important which will reduce the amplifying effect in real systems. The non-linear Schrödinger equation in one-dimension reads

$$i\hbar\frac{\partial\psi(x,t)}{\partial t}=\frac{-\hbar^2}{2m}\frac{\partial^2\psi(x,t)}{\partial x^2}+\left(\left|\psi(x,t)\right|^2+V(x)\right)\psi(x,t) \tag{7.1}$$

It is also expected that dispersion will play a major role in the real lasing systems and consequently its inclusion will be of great benefit.

REFERENCES

1. H. Bahlouli, A. D. Alhaidari, and A. Al Zahrani E. N. Economou. Phys. Rev. Lett. B (2005). (In Press)
2. Jiang X., Li Q and Soukoulis C. M., Phys. Rev. B Vol. 59, 9007 (1999).
3. Ma Xiaozheng., Soukoulis C. M., Physica B Vol. 296, 107 (2001).
4. S. Ramakrishna and A. Armour, Am. J. Phys. 71 (6), June 2003.
5. D. Schneble, et al, cond-mat/0311138. November 6, 2003
6. Genack A. Z. and Drack D. M., Nature Vol. 368, 400 (1994).
7. Lawandy N. M., Balachandran R. M., Gomes A. S. L., van Albada M. P. and Lagendijk A. Phys. Rev. Lett. Vol. 75, 1739 (1995).
8. Freilikher V., Pustilnik M. And Yurkevich I., Phys. Rev. Lett. 73, 810 (1994).
9. Beenakker C. W., Paasschens J. C. J. And Brouwer P. W., Phys. Rev. Lett. Vol. 76, 1368 (1996).
10. Zekri N., Bahlouli H. And Sen A., J. Phys.: Condense. Matter Vol. 10, 2405 (1998).
11. Prabhakar Pradhan and N. Kumar, Phys. Rev. B 50, 9644 (1994).
12. Zhang Z. Q., Phys. Rev. B Vol. 52, 7960 (1995).
13. Qiming Li, K.H. Ho and C.M. Soukoulis, Physica B 296, 78 (2001).
14. W. Greiner, Relativistic Quantum Mechanics: Wave Equation, 3rd edition. Springer, Berlin, 2000.
15. J. D. Bjorken and S. D. Drell, Relativistic Quantum Mechanics. McGraw-Hill, New York, 1964.
16. C. Y. Chen, D. S. Sun and F. L. Lu, Phys. Lett. A 330, 424 (2004).
17. C. Y. Chen, C. L. Liu, F. L. Lu and D. S. Sun, Acta Phys. Sin. 52, 1579 (2003).
18. C. L. Hammer, T. A. Weber, and V. S. Zidell, Am. J. Phys. 45, 933 (1977).
19. J. D. Jackson, Classical Electrodynamics, 3rd edition. John Wiley & Sons, Inc., 1999.
20. R. Liboff, Quantum Mechanics, 3rd edition. Addison Wesley 1996.
21. S. Bandyopadhyay, A. S. Majumdar and D. Home, arXiv: guant-ph/0103001 v2 21 Aug 2001.
22. J. Paasschens, et al Phys. Rev. B. Vol. 54, 11887 (1996).
23. R. Burden and J. Faires, Numerical Analysis, 7th edition. Brooks/Cole 2001.
24. W. Ames, Numerical methods for partial differential equations, 3rd edition. Academic Press 1992.
25. A. Goldberg, H. Schey, and J Schwartz, 35 (3), 177-186(1967).
26. R. Lombard, J. Mares and C. Volpe. arXiv:hep-ph/0411067 v1 4 Nov 2004.
27. D. Griffiths, Introduction to Electrodynamics, 3rd edition, Prentice Hall 1996.
28. C. Bender, D. Brody, and H. Jones. Am. J. Phys., Vol. 71, No. 11, November 2003

VITA

- Abdallah Muhammad Al Zahrani
- Born in Jeddah, Saudi Arabia
- Received B.Sc. in Physics in June 5, 2002, King Fahd University of Petroleum and minerals, Dhahran, Saudi Arabia.